Photon emission from slightly roughened tunnel junctions

Bernardo Laks* and D. L. Mills
Department of Physics, University of California, Irvine, California 92717
(Received 19 July 1979)

In this paper, we derive expressions for the distribution in angle and frequency of electromagnetic radiation emitted from fluctuations in the tunneling current between two metals separated by a thin oxide barrier. The calculation provides an explicit description of the decoupling of the surface polariton from the surface by virtue of small-amplitude roughness present there. In addition, we find radiation from direct coupling of current fluctuations in the junction structure to the transverse radiation field. Numerical calculations are presented which explore the predictions of the theory, when applied to structures similar to those studied experimentally by Lambe and McCarthy. We suggest interpretations of some features of their data, and data reported by Adams, Wyss, and Hansma. The theory indicates that as the amplitude of the roughness is increased, the quantum efficiency of the device should saturate to approach a value independent of the roughness amplitude.

I. INTRODUCTION

In a series of recent experiments, the emission of light from tunnel junctions has been reported, and a number of its characteristics have been studied.[1] The junctions consist of two normal (i.e., nonsuperconducting) metals separated by a thin oxide barrier some 20 or 30 Å in thickness. Low temperatures are not required to observe the phenomenon. Indeed, in a darkened room, the emitted radiation from room-temperature devices can be seen by the naked eye.[2] Finally, the radiation has a broad spectral distribution that cuts off at the frequency $\nu_c = eV_0/h$, where V_0 is the bias voltage.

In all of the experiments, the outer surface of the device is either roughened, or small particles are deposited upon the oxide layer. The intensity of emitted radiation is clearly larger for such nonuniform surface geometries that in the case where all surfaces are nominally smooth. At the same time, Lambe and McCarthy[3] report a saturation of the intensity emitted with increased amplitude of the roughness.

For slightly roughened surfaces, Lambe and McCarthy[1] proposed a two-step process which they suggest is responsible for the light emission. As the electron tunnels through the barrier, it may do so inelastically with emission of a surface polariton bound to the metal-oxide-metal interface. Such a wave cannot radiate, but may decouple from the surface if roughness is present.[4]

The present investigation was motivated by the desire to construct a detailed theory of this second-order process, in the limit of small amplitude roughness. We proceed by solving Maxwells equations for the radiation produced by fluctuations in time of the tunneling current. The effect of roughness is treated by a perturbation theoretic method based on recent Green's function approaches to the study of surface roughness effects.[5] The coupling of tunneling electrons to the surface polariton has been discussed recently by Davis,[6] who examined this for two metals each of semi-infinite extend separated by an oxide barrier. However, in his theory, Davis did not address the manner in which surface roughness converts the surface polariton to radiation. As a result, his paper is not able to provide a quantitative description of the intensity of the emitted radiation, nor an account of how various parameters that characterize the roughness influence the spectral composition of the light.

In a sequence of papers,[7] Scalapino and his collaborators address the spectrum of light emitted from a spherical particle set on top of an oxide layer formed on a flat metallic surface. One may view our study and their work as complementary, in that we explore the effect of roughness in the limit that its amplitude is small, while they are concerned with the opposite extreme of globular objects on top of the oxide. We shall see that certain features of our calculated spectra are similar to theirs, but there are also clear and distinct differences, most particularly with respect to the polarization properties of the emitted radiation.

It may prove helpful to list some of our principal conclusions in this introductory section.

(i) While optical experiments indicate the transverse correlation length associated with roughened surfaces are the order of 400 Å or so,[8] for films deposited on CaF_2 substrates, we require transverse correlation lengths an order of magnitude smaller to generate spectra similar to the data. Thus, from the tunneling experiments, one can obtain information about the distribution of roughness on the length scale of a few tens of Angstroms, which are

too small to affect optical measurements.

(ii) The second-order process suggested by Lambe and McCarthy produces a spectrum of emitted radiation that does not extend to frequencies beyond the maximum surface polariton frequency, save for a small tail. For Al-Al_2O_3-Au junctions, this cutoff frequency is around 2.2 eV. Yet in much of the data reported, the measured spectrum extends right up to $\nu_c = eV_0/h$, even when V_0 is well above 2.2 V.[9] We have also investigated direct emission of radiative photons by the fluctuations in tunnel current, to find this process competitive in strength with the second-order roughness-induced process proposed by Lambe and McCarthy for frequencies in the visible, were Au has strong interband optical transitions. This is for Al-Al_2O_3-Au junctions and parameters relevant to junctions employed by Lambe and McCarthy. For a junction composed of a Ag overlayer rather than Au, the direct emission is expected to be weak for voltages below ≈ 4 V where interband transitions do not influence the optical response of Ag. Thus, it would be of considerable interest to see data on Al-Al_2O_3-Ag junctions for voltages beyond the 3.5 eV cutoff of the surface polariton branch of this structure.

(iii) In theoretical work of Scalapino and coworkers, it is presumed that the electromagnetic field is driven only by the tunnel current fluctuations within the oxide barrier. If we use such a picture, the tunneling efficiency is smaller than that estimated experimentally by some two orders of magnitude. In fact, fluctuations in the tunnel current must extend throughout the junction structure, in our view, and the fluctuations within the metal also couple to the surface polariton, since its electric fields are nonzero there also. A simple model of coupling between current fluctuations in the metal to the surface polariton produces a tunneling efficiency comparable in magnitude to that observed.

(iv) We explore also the influence of the thickness of the outer metal on the tunneling efficiency, for parameters characteristic of the devices employed by Lambe and McCarthy. The finite thickness strongly modifies the surface polariton dispersion relation at long wavelengths, but there is no dramatic effect on the emission spectra, in the frequency range explored to date.

(v) Our description of the second-order roughness induced radiation process shows the emitted intensity to be proportional to the square of the amplitude of the roughness δ^2, and also to the mean free path of the surface polariton $l(\omega)$. If in the formula, we replace $l(\omega)$ by the form appropriate to a surface wave on a rough surface,[10] then as the amplitude increases, so $l(\omega) \sim \delta^{-2}$ in simplest approximation, we expect a saturation of the emitted light intensity. Such a saturation effect has been reported by Lambe and McCarthy, who suggest the saturation results because the surface polariton acquires a short lifetime on a rough surface. In effect, our calculation shows how this can emerge from a detailed theory. Presently calculations of the roughness contribution to $I(\omega)$ are underway for the geometries of interest here. These will be discussed in a subsequent publication.

The outline of this paper is as follows. In Sec. II, we develop the expressions for the distribution in frequency and angle of the radiation emitted by current fluctuations in a junction structure with slightly roughened outer surface. Section III reports and discusses the numerical calculations on which the above conclusions are based.

II. THEORETICAL DISCUSSION

The geometry we consider is illustrated in Fig. 1. We consider a semi-infinite substrate with dielectric constant $\epsilon_3(\omega)$, which in general is complex. The substrate is overlaid with an oxide layer of thickness d, and this by a film of nominal thickness L. The dielectric constant of the oxide layer is $\epsilon_2(\omega)$ and that of the film is $\epsilon_1(\omega)$. The z axis of the coordinate system is normal to the surface of the substrate, and its surface coincides with the x-y plane. Finally, the surface of the outer film is roughened. The location of a point on the surface is defined by the relation $z = L + d + \zeta(\vec{x}_\parallel)$, with $\vec{x}_\parallel = x\hat{x} + y\hat{y}$. The function $\zeta(\vec{x}_\parallel)$ thus describes the roughness on the outer surface, and if angular brackets denote a statistical average over possible profiles for the roughness, we define $\zeta(\vec{x}_\parallel)$ so that $\langle\zeta(\vec{x}_\parallel)\rangle = 0$. Also $\delta^2 = \langle\zeta^2(\vec{x}_\parallel)\rangle$ is the rms deviation of the outer surface from perfect flatness. We do ignore the influence of the finite thickness of the substrate; the formalism here can be readily extended to include this, at the price of algebraic complexity. We believe the finite thickness of the substrate has only a minor influence on the

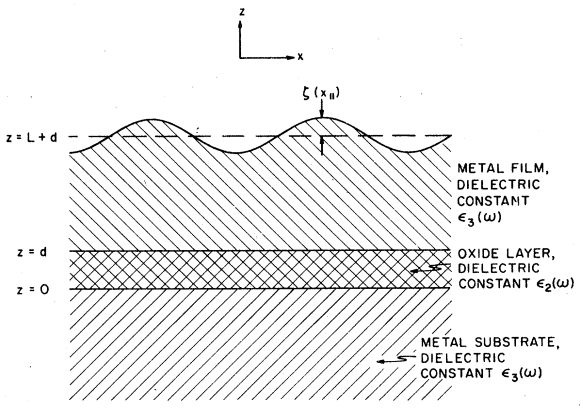

FIG. 1. Geometry analyzed in the present paper. We have a semi-infinite substrate overlaid with an oxide barrier of thickness d, and a metal film of nominal thickness L above. The surface of the upper film is roughened.

results, as long as its thickness is larger than the skin depth at the frequency of the emitted radiation.

We now suppose a dc voltage V_0 is put across the junction. This causes a dc current density J_0 to flow through the oxide barrier. Superimposed on the dc current are fluctuations in current density $\vec{J}(\vec{x},t)$. It is these fluctuations that lead to the radiation field. Later on we shall model the spectrum of current fluctuations, following the approach used by Scalapino and collaborators. For the moment, we assume $\vec{J}(\vec{x},t)$ to be known and we address the question of calculating the intensity of the radiation emitted by the structure.

If we Fourier transform the current fluctuations by writing

$$J_\mu(\vec{x},t)=\int_{-\infty}^{+\infty}\frac{d\omega}{2\pi}J_\mu(\vec{x};\omega)e^{-i\omega t}\ , \tag{2.1}$$

then the amplitude $E_\mu(\vec{x};\omega)$ of the electric field component at frequency ω, and position $\vec{x}$ can be written in terms of a set of Green's functions $D_{\mu\nu}(\vec{x},\vec{x}';\omega)$ similar to those introduced in earlier work.[5] We have

$$E_\mu(\vec{x},\omega)=i\frac{\omega}{c^2}\sum_\lambda\int d^3x'\,D_{\mu\lambda}(\vec{x},\vec{x}';\omega)\,J_\lambda(\vec{x}',\omega)\ , \tag{2.2}$$

where as earlier, Green's functions are constructed as the solution of the matrix of equations

$$\sum_\mu\left[\frac{\omega^2}{c^2}\epsilon(\vec{x},\omega)\delta_{\lambda\mu}-\frac{\partial^2}{\partial x_\lambda\partial x_\mu}+\delta_{\lambda\mu}\nabla^2\right]D_{\mu\nu}(\vec{x},\vec{x}';\omega)$$

$$=4\pi\delta_{\lambda\mu}\delta(\vec{x}-\vec{x}')\ . \tag{2.3}$$

The matrix of Green's functions constructed for Eq. (2.3) are those for the geometry illustrated in Fig. 1, for which the outer surface is roughened. For fixed $\vec{x}'$, as $|\vec{x}|\to\infty$ in the vacuum above the structure, the outgoing wave boundary condition is imposed, while as $|\vec{x}|\to\infty$ in a direction that takes one into the substrate, Green's functions vanish. We shall give the explicit form of the elements of Green's-function matrix in the discussion below.

It is convenient to transform out the spatial variation of Green's functions in the two directions parallel to the surface. We do this by writing

$$D_{\mu\lambda}(\vec{x}\vec{x}';\omega)=\int\frac{d^2k_\parallel d^2k'_\parallel}{(2\pi)^4}\,e^{i\vec{k}_\parallel\cdot\vec{x}_\parallel}e^{-i\vec{k}'_\parallel\cdot\vec{x}'_\parallel}$$

$$\times D_{\mu\lambda}(\vec{k}_\parallel,\vec{k}'_\parallel;zz';\omega)\ . \tag{2.4}$$

Here $\vec{x}_\parallel$ is the projection of $\vec{x}$ onto the x-y plane.

Furthermore, we need the electric field in the vacuum above the structure to calculate the intensity of the emitted radiation, so we want to examine the behavior of $E_\mu(\vec{x},\omega)$ as $z\to+\infty$. If we define

$$k_0=\left[\frac{(\omega+i\eta)^2}{c^2}\right]^{1/2}\ , \tag{2.5}$$

with η a positive infinitesmal, and choose the square root with $\mathrm{Im}(k_0)>0$ always, then for z in the vacuum above the structure, the outgoing wave boundary condition insures that $D_{\mu\lambda}(\vec{k}_\parallel,\vec{k}'_\parallel;zz';\omega)$ has the form

$$D_{\mu\lambda}(\vec{k}_\parallel,\vec{k}'_\parallel;zz';\omega)=e^{ik_0z}\epsilon_{\mu\lambda}(\vec{k}_\parallel,\vec{k}'_\parallel;z';\omega)\ . \tag{2.6}$$

Thus, we can write, for z in the vacuum above the film,

$$E_\mu(\vec{x},\omega)=i\frac{\omega}{c^2(2\pi)^4}\int d^2k_\parallel e^{i\vec{k}_\parallel\cdot\vec{x}_\parallel}e^{ik_0z}$$

$$\times\sum_{\lambda'}\int d^2k'_\parallel d^3x'e^{-i\vec{k}'_\parallel\cdot\vec{x}'_\parallel}$$

$$\times\epsilon_{\mu\lambda}(\vec{k}_\parallel\vec{k}'_\parallel;z';\omega)J_\lambda(\vec{x}';\omega)\ . \tag{2.7}$$

In the integral on $\vec{k}_\parallel$, which covers all values of the wave vector, it is only the regime with $k_\parallel<\omega/c$ that describes radiation emitted from the surface. Here k_0 is real and positive as η tends to zero. When $k_\parallel>\omega/c$, we obtain a description of radiation fields localized in the near vicinity of surface, since as $\eta\to0$, k_0 is pure imaginary with positive imaginary part. Thus for our purposes, since only the radiation emitted from the junction is of interest, we split the integral on $\vec{k}_\parallel$ into two parts by writing

$$\int d^2k_\parallel=\int_{|\vec{k}_\parallel|<\omega/c}d^2k_\parallel+\int_{|\vec{k}_\parallel|>\omega/c}d^2k_\parallel \tag{2.8}$$

and we discard the contribution from the regime $|\vec{k}_\parallel|>\omega/c$.

As $|\vec{x}|\to\infty$, with z positive, a steepest descents method can be used to evaluate the integral on $\vec{k}_\parallel$. We can write

$$\vec{x}=\vec{x}_\parallel+\hat{z}z$$

$$=|\vec{x}|(\sin\theta_0\cos\phi_0\,\hat{x}+\sin\theta_0\sin\phi_0\,\hat{y}+\cos\theta_0\,\hat{z}) \tag{2.9}$$

and also let

$$\vec{k}_\parallel=\frac{\omega}{c}(\sin\theta\cos\phi\,\hat{x}+\sin\theta\sin\phi\,\hat{y})\ , \tag{2.10a}$$

which gives for $\omega<ck_\parallel$

$$k_0=\frac{\omega}{c}\cos\theta\ . \tag{2.10b}$$

Note that since k_0 must be positive, we have $0\le\theta\le\frac{1}{2}\pi$. The integral on $\vec{k}_\parallel$ may then be con-

verted to one on θ and ϕ to give

$$E_\mu^{(R)}(\vec{x},\omega)=\frac{i\omega^3}{16\pi^4c^4}\int d\theta\,d\phi\sin\theta\cos\theta\,e^{i\vec{k}\cdot\vec{x}}\sum_\lambda\int d^2k_\parallel' d^3x'\,e^{-i\vec{k}_\parallel'\cdot\vec{x}_\parallel'}\epsilon_{\mu\lambda}(\vec{k}_\parallel\vec{k}_\parallel';z';\omega)J_\lambda(\vec{x}';\omega)\ . \tag{2.11}$$

We have

$$\vec{k}\cdot\vec{x}=\frac{\omega}{c}|\vec{x}|[\sin\theta\sin\theta_0\cos(\phi-\phi_0)+\cos\theta\cos\theta_0]\ , \tag{2.12}$$

which has an extremum when $\phi=\phi_0$ and $\theta=\theta_0$. Thus, as $|\vec{x}|\to\infty$, the contributions in the θ and ϕ integrals come only from the near vicinity of θ_0 and ϕ_0. The integral may then be evaluated by expanding $\vec{k}\cdot\vec{x}$ in powers of $(\theta-\theta_0)$ and $(\phi-\phi_0)$, retaining up to terms quadratic in these small deviations from the direction of observation. Then as this is done, in all the remaining quantities in the integrand which vary slowly with $\vec{k}_\parallel$, we replace $\vec{k}_\parallel$ by $\vec{k}_\parallel^{(0)}$, where

$$\vec{k}_\parallel^{(0)}=\frac{\omega}{c}\sin\theta_0(\hat{x}\cos\phi_0+\hat{y}\sin\phi_0)\ . \tag{2.13}$$

The procedure is the same as that used in an earlier discussion of the finite mean free path of surface polaritons in the presence of surface roughness.[4] Then as $z\to+\infty$, this gives for the radiated component $E_\mu^{(R)}(\vec{x},\omega)$ of the outgoing electric field the expression

$$E_\mu^{(R)}(\vec{x},\omega)=i\frac{\omega^2\cos\theta_0}{8\pi^3c^3}\frac{\exp[i\omega/c|\vec{x}|]}{|\vec{x}|}\sum_\lambda\int d^2k_\parallel'\,d^3x'\,e^{-i\vec{k}_\parallel'\cdot\vec{x}_\parallel'}\epsilon_{\mu\lambda}(\vec{k}_\parallel^{(0)},\vec{k}_\parallel';z';\omega)\,J_\lambda(\vec{x}',\omega)\ . \tag{2.14}$$

The energy per unit solid angle, per unit time, per unit frequency that is emitted in the direction specified by the angles (θ_0,ϕ_0) is given by $|\vec{x}|^2\langle S\rangle$, where $\langle S\rangle$ is the magnitude of the time-averaged Poynting vector

$$\langle S\rangle=\frac{c}{8\pi}\sum_\mu\langle E_\mu^{(R)}(\vec{x},\omega)^*E_\mu^{(R)}(\vec{x},\omega)\rangle\ . \tag{2.15}$$

Thus, if $d^3W/d\Omega\,d\omega\,dt$ is the energy radiated per unit time, per unit solid angle $d\Omega$, we have

$$\frac{d^3W}{d\Omega\,d\omega\,dt}=\frac{\omega^4\cos^2\theta_0}{512\pi^7c^5}\sum_{\lambda\lambda'}\sum_\mu\int d^2k_\parallel'\,d^2k_\parallel''\,d^3x'\,d^3x''\,e^{-i\vec{k}_\parallel'\cdot\vec{x}_\parallel'}e^{+i\vec{k}_\parallel''\cdot\vec{x}_\parallel''}\epsilon_{\mu\lambda'}(\vec{k}_\parallel^{(0)},\vec{k}_\parallel';z';\omega)^*\epsilon_{\mu\lambda'}(\vec{k}_\parallel^{(0)},\vec{k}_\parallel'';z'';\omega)$$
$$\times\langle J_\lambda^*(\vec{x}',\omega)J_{\lambda'}(\vec{x}'',\omega)\rangle\ . \tag{2.16}$$

The angular brackets denote a statistical average over the current fluctuations in the junction, biased by the dc voltage V_0. We presume the current fluctuation spectrum is well approximated by that in a structure with smooth, perfectly flat outer surface, in the spirit of the present paper which treats the roughness as a small perturbation. We then write

$$\langle J_\lambda^*(\vec{x}',\omega)J_{\lambda'}(\vec{x}'',\omega)\rangle=\int d^2Q_\parallel e^{+\vec{Q}_\parallel\cdot(\vec{x}_\parallel'-\vec{x}_\parallel'')}J_{\lambda\lambda'}(\vec{Q}_\parallel\omega;z'z'') \tag{2.17}$$

to take advantage of translational invariance parallel to the surface, and Eq. (2.16) becomes

$$\frac{d^3W}{d\Omega\,d\omega\,dt}=\frac{\omega^4\cos^2\theta_0}{32\pi^3c^5}\int d^2Q_\parallel\,dz'\,dz''\sum_\mu\sum_{\lambda\lambda'}\epsilon_{\mu\lambda}(\vec{k}_\parallel^{(0)},\vec{Q}_\parallel;z';\omega)^*\epsilon_{\mu\lambda'}(\vec{k}_\parallel^{(0)},\vec{Q}_\parallel;z'';\omega)\mathcal{J}_{\lambda\lambda'}(\vec{Q}_\parallel\omega;z'z'')\ . \tag{2.18}$$

We must next turn to the construction of the functions $\epsilon_{\mu\lambda}(\vec{k}_\parallel^{(0)}\vec{Q}_\parallel;z';\omega)$, which are related to the electromagnetic Green's function matrix as specified in Eqs. (2.4) and (2.6). We shall proceed by treating the roughness in perturbation theory, and expanding Green's functions in powers of $\delta^2=\langle\zeta^2(\vec{x}_\parallel)\rangle$, to retain the first nonvanishing contribution to Eq. (2.18).

As remarked in Sec. I, we also find an appreciable amount of radiation from the junction even when $\delta^2=0$ and the outer surface is smooth. We first derive the contribution to the radiation intensity of order δ^2, then after this completed, we turn to the discussion of radiation from a structure with perfectly smooth surfaces.

The dielectric function $\epsilon(\vec{x}, \omega)$ in Eq. (2.3) may be split into two parts

$$\epsilon(\vec{x}, \omega) = \epsilon^{(0)}(z, \omega) + \Delta\epsilon(\vec{x}, \omega) \quad . \tag{2.19}$$

Here $\epsilon^{(0)}(z, \omega)$ is the dielectric function for the three layer structure with smooth surfaces [so $\epsilon^{(0)}(z, \omega)$ is a function only of z] while $\Delta\epsilon(\vec{x}, \omega)$ is the change in the dielectric constant produced by the roughness. If $\Theta(\xi)$ is the step function equal to unity for positive values of its argument and zero for negative values, we have the explicit form

$$\begin{aligned}\Delta\epsilon(\vec{x}, \omega) = \epsilon_1(\omega)[&\Theta(L + d + \zeta(\vec{x}_\parallel) - z) \\ &- \Theta(L + d - z)] \\ &+ [\Theta(z - L - d - \zeta(\vec{x}_\parallel)) - \Theta(z - L - d)] \quad .\end{aligned} \tag{2.20}$$

Then if $D^{(0)}_{\mu\lambda}(\vec{x}\vec{x}';\omega)$ are Green's functions for the structure with perfectly smooth surfaces, Eq. (2.3) may be converted to an integral equation

$$\begin{aligned}D_{\mu\nu}(\vec{x}, \vec{x}';\omega) = D^{(0)}_{\mu\nu}(\vec{x}, \vec{x}';\omega) \\ - \frac{\omega^2}{4\pi c^2} \sum_\lambda \int d^3x'' \, D^{(0)}_{\mu\lambda}(\vec{x}\vec{x}'';\omega) \\ \times \Delta\epsilon(\vec{x}'', \omega) D_{\lambda\nu}(\vec{x}''\vec{x}';\omega) \quad .\end{aligned} \tag{2.21}$$

Through iteration of Eq. (2.21), we obtain the first correction to the smooth surface Green's-function matrix $D^{(0)}_{\mu\nu}(\vec{x}, \vec{x}';\omega)$. If we call this correction $D^{(1)}_{\mu\nu}(\vec{x}\vec{x}';\omega)$ then

$$\begin{aligned}D^{(1)}_{\mu\nu}(\vec{x}\vec{x}';\omega) = &- \frac{\omega^2}{4\pi c^2}[\epsilon_1(\omega) - 1] \\ &\times \int d^2x''_\parallel \int_{L+d}^{L+d+\zeta(\vec{x}''_\parallel)} dz'' \sum_\lambda D^{(0)}_{\mu\lambda}(\vec{x}\vec{x}'';\omega) \\ &\times D_{\lambda\nu}(\vec{x}''\vec{x}', \omega) \quad .\end{aligned} \tag{2.22}$$

As Agarwal has pointed out,[5] the limit $\zeta(\vec{x}_\parallel)$ must be taken carefully in Eq. (2.22), since $D^{(0)}_{\mu\lambda}(\vec{x}\,\vec{x}'';\omega)$ and $D^{(0)}_{\lambda\nu}(\vec{x}''\vec{x}';\omega)$ both have jump discontinuities across the surface $z' = L + d$, when the index λ refers to the z directions. We take the limit $\zeta(\vec{x}_\parallel) \to 0$ through use of a simple version of Agarwal's argument; this avoids an error that appeared at one point in an early application of Green's-function method to the roughness problem.[11]

To proceed, we note that those elements of $D^{(0)}_{\mu\lambda}$ which suffer a jump discontinuity do so across $z = L + d$, while the elements of the full Green's $D_{\mu\lambda}$ matrix suffer a jump discontinuity not across this surface, but rather across the actual rough surface defined by $z = L + d + \zeta(\vec{x}_\parallel)$. Consider a point $\vec{x}''_\parallel$ where $\zeta(\vec{x}''_\parallel) > 0$. All points z'' in the integration lie *above* the surface $z'' = L + d$, so for small $\zeta(\vec{x}''_\parallel)$ we may replace z'' by $z'' = (L + d) +$ in $D^{(0)}_{\mu\lambda}$. The full Green's function, on the other hand, is evaluated *below* the surface of discontinuity, with z'' in the outer film. Thus, to first approximation we replace $D_{\lambda\mu}(\vec{x}''\vec{x}', \omega)$ by $D^{(0)}_{\lambda\nu}(\vec{x}''\vec{x}', \omega)$ but with $z'' = (L + d)-$, in the lower medium. When $\zeta(\vec{x}_\parallel) < 0$, we proceed in the opposite way, by replacing z' by $(L + d) -$ in $D^{(0)}_{\mu\lambda}$. But it is a consequence of the electromagnetic boundary conditions that

$$D^{(0)}_{\mu\lambda}(\vec{x}_\parallel z, \vec{x}''_\parallel(L + d) +;\omega) D^{(0)}_{\lambda\nu}(\vec{x}''_\parallel(L + d) -, \vec{x}'_\parallel z';\omega) \equiv D^{(0)}_{\mu\lambda}(\vec{x}_\parallel z, \vec{x}''_\parallel(L + d) -;\omega) D^{(0)}_{\lambda\nu}(\vec{x}''_\parallel(L + d) +, \vec{x}'_\parallel z';\omega) \tag{2.23}$$

so the same replacement may be employed for both signs of $\zeta(\vec{x}_\parallel)$. Then for the correction to Green's matrix first order in the roughness, we have

$$D^{(1)}_{\mu\nu}(\vec{x}_\parallel z, \vec{x}_\parallel' z';\omega) = - \frac{\omega^2}{4\pi c^2}[\epsilon_1(\omega) - 1] \int d^2x''_\parallel \, \zeta(\vec{x}''_\parallel) \sum_\lambda D^{(0)}_{\mu\lambda}(\vec{x}_\parallel z, \vec{x}''(L + d) +;\omega) D^{(0)}_{\lambda\mu}(\vec{x}''_\parallel(L + d) -, \vec{x}'_\parallel z';\omega) \quad . \tag{2.24}$$

Now, as in earlier papers, for the smooth surface Green's functions, we may take advantage of translational invariance in the two directions in the surface by writing

$$D^{(0)}_{\mu}(\vec{x}\vec{x}';\omega) = \int \frac{d^2k_\parallel}{(2\pi)^2} e^{i\vec{k}_\parallel \cdot (\vec{x}_\parallel - \vec{x}'_\parallel)} d^{(0)}_{\mu\nu}(\vec{k}_\parallel \omega | zz') \quad . \tag{2.25}$$

Then to first order in the amplitude of the surface roughness, we have for the quantity $D_{\mu\nu}(\vec{k}_\parallel \vec{k}'_\parallel; zz';\omega)$ defined in Eq. (2.4) the expression

$$D^{(1)}_{\mu\nu}(\vec{k}_\parallel \vec{k}'_\parallel; zz';\omega) = - \frac{\omega^2[\epsilon_1(\omega) - 1]}{4\pi c^2} \zeta(\vec{k}_\parallel - \vec{k}'_\parallel) \sum_\lambda d^{(0)}_{\mu\lambda}(\vec{k}_\parallel \omega | z, (L + d) +) d^{(0)}_{\lambda\nu}(\vec{k}'_\parallel \omega | (L + d) -, z') \quad . \tag{2.26}$$

For the structure illustrated in Fig. 1, the explicit form of the functions $d^{(0)}_{\mu\nu}(\vec{k}_\parallel \omega | zz')$ is given in the Appendix of the present paper.

Finally, we note it is only the limit $z > (L+d)$ that is relevant for our discussion of the radiation emitted by the junction structure. For $z > 0$, we may write

$$d_{\mu\lambda}^{(0)}(\vec{k}_{\parallel}\omega|z,(L+d)+) = e^{+ik_0^z}\gamma_{\mu\lambda}(\vec{k}_{\parallel}\omega) \tag{2.27}$$

When this is followed through to the expression for the intensity of the emitted radiation, we have

$$\frac{d^3W}{d\Omega\, d\omega\, dt} = \frac{\omega^8|\epsilon_1(\omega)-1|^2\cos^2\theta_0}{512\pi^5c^9}\sum_{\mu}\sum_{\lambda\lambda'}\sum_{\eta\eta'}\gamma_{\mu\eta}^*(\vec{k}_{\parallel}^{(0)},\omega)\gamma_{\mu\eta'}(\vec{k}_{\parallel}^{(0)},\omega)$$
$$\times\int d^2Q_{\parallel}\,|\zeta(\vec{k}_{\parallel}^{(0)}-\vec{Q}_{\parallel})|^2\int dz'\,dz''\,d_{\eta\lambda}^{(0)}(\vec{Q}_{\parallel}\omega||(L+d)-,z')^*$$
$$\times d_{\eta\lambda'}^{(0)}(\vec{Q}_{\parallel}\omega|(L+d)-,z'')\mathcal{J}_{\lambda\lambda'}(\vec{Q}_{\parallel}\omega|z'z'')\ . \tag{2.28}$$

For the case of interest here, where the roughness on the outer surface is random in nature, a simplification of Eq. (2.28) may be achieved without loss of generality. Suppose we let $\vec{k}^{(0)}$ be the wave vector of the radiation emitted by the system. Let $\vec{k}^{(0)}$ make the angle θ_0 with the z axis, and its projection on the xy plane make the angle ϕ_0 with respect to the x axis, as assumed in Eq. (2.13). In the $\vec{Q}_{\parallel}$ integration, with $\theta_{Q_{\parallel}}$ the angle between $\vec{Q}_{\parallel}$ and the x axis, we have $d^2Q_{\parallel} = d\theta_{Q_{\parallel}}\,dQ_{\parallel}\,Q_{\parallel}$. Quite clearly, after integration on $\theta_{Q_{\parallel}}$, the angular distribution of the radiation must be independent of ϕ_0 and depend on only θ_0. Then if we average Eq. (2.28) over ϕ_0 by multiplying by $\int_0^{2\pi} d\phi_0/2\pi$, the answer remains unchanged. If we do this, then interchange the order of integration on ϕ_0 with that on $\vec{k}_{\parallel}^{(0)}$, we have

$$\frac{d^3W}{d\Omega\, d\omega\, dt} = \frac{\omega^8|\epsilon_1(\omega)-1|^2\cos^2\theta_0}{512\pi^5c^9}\sum_{\mu}\sum_{\lambda\lambda'}\sum_{\eta\eta'}\int d^2Q_{\parallel}\,dz\,dz'\,d_{\eta\lambda}^{(0)}(\vec{Q}_{\parallel}\omega|(L+d)-,z')^*\,d_{\eta\lambda'}^{(0)}(\vec{Q}_{\parallel}\omega|(L+d)-,z'')$$
$$\times\mathcal{J}_{\lambda\lambda'}(\vec{Q}_{\parallel}\omega|z'z'')\langle|\zeta(\vec{k}_{\parallel}^{(0)}-\vec{Q}_{\parallel})|^2\gamma_{\mu\eta}^*(\vec{k}_{\parallel}^{(0)},\omega)\gamma_{\mu\eta'}(\vec{k}_{\parallel}^{(0)},\omega)\rangle\ , \tag{2.29}$$

where the angular brackets denote an average on the angle ϕ_0. Now after this average is performed, symmetry considerations show the integrand must be independent of the *direction* of $\vec{Q}_{\parallel}$, and it depends on only its magnitude. Hence, we can evaluate the integrand by choosing $\vec{Q}_{\parallel}$ to be directed along a selected direction, say along $\hat{x}$. After this is done, the integration on $\theta_{Q_{\parallel}}$ gives a factor of 2π, while the quantities $d_{\eta\lambda}^{(0)}(\vec{Q}_{\parallel}\omega|(L+d)-z')$ are replaced by the much simpler of quantities $g_{\eta\lambda}^{(0)}(Q_{\parallel}\omega|(L+d)-z)$ defined in the Appendix.

After $\vec{Q}_{\parallel}$ is replaced by $\hat{x}Q_{\parallel}$, one notes that charge density fluctuations render nonzero those $\mathcal{J}_{\lambda\lambda'}(\hat{x}Q_{\parallel}\omega|zz')$ with λ or λ' equal to x or z. When these simplifications are combined with the explicit expressions for Green's-function elements $g_{\eta\lambda}(Q_{\parallel}\omega|(L+d)-,z)$, after a rather lengthy algebraic reduction, we find Eq. (2.29) may be cast in the form

$$\frac{d^3W}{d\Omega\, d\omega\, dt} = \frac{8\omega^2|\epsilon_1(\omega)-1|^2}{\pi c^3}\int_0^{2\pi}d\phi_0\int_0^{\infty}\frac{dQ_{\parallel}\,Q_{\parallel}|\zeta(\vec{k}_{\parallel}^{(0)}-\hat{x}Q_{\parallel})|^2}{|D(Q_{\parallel},\omega)|^2}\exp[-2k_0^{(I)}(Q_{\parallel},\omega)(L+d)]$$
$$\times\left\{|k_0(Q_{\parallel},\omega)|^2|r_y(k_{\parallel}^{(0)},\omega)|^2\sin^2\phi_0\right.$$
$$\left.+\left|k_0(Q_{\parallel},\omega)r_x(k_{\parallel}^{(0)},\omega)\cos\theta_0\cos\phi_0-\frac{Q_{\parallel}}{\epsilon_1(\omega)}r_z(k_{\parallel}^{(0)},\omega)\sin\theta_0\right|^2\right\}$$
$$\times\int dz\,dz'\,[E_x^{<}(Q_{\parallel}\omega|z)^*E_x^{<}(Q_{\parallel}\omega|z')\mathcal{J}_{xx}(Q_{\parallel}\omega|zz')$$
$$-E_z^{<}(Q_{\parallel}\omega|z)^*E_x^{<}(Q_{\parallel}\omega|z')\mathcal{J}_{zx}(Q_{\parallel}\omega|zz')$$
$$-E_x^{<}(Q_{\parallel}\omega|z)^*E_z^{<}(Q_{\parallel}\omega|z')\mathcal{J}_{xz}(Q_{\parallel}\omega|zz')$$
$$+E_z^{<}(Q_{\parallel}\omega|z)^*E_z^{<}(Q_{\parallel}\omega|z')\mathcal{J}_{zz}(Q_{\parallel}\omega|zz')]\ . \tag{2.30}$$

In Eq. (2.30),

$$k_0(Q_{\parallel},\omega)=[(\omega+i\eta)^2/c^2-Q_{\parallel}^2]^{1/2}$$

with $k_0^{(I)}(Q_{\parallel},\omega)=\mathrm{Im}[k_0(Q_{\parallel},\omega)]>0$, and we have defined

$$D(Q_{\parallel},\omega)=\left[\left(\epsilon_3-\frac{k_3}{k_0}\right)\cos(k_2d)\cos(k_1L)+i\left(\epsilon_1\frac{k_3}{k_1}-\frac{k_1\epsilon_3}{k_0\epsilon_1}\right)\cos(k_2d)\sin(k_1L)\right.$$
$$+i\left(\frac{k_3\epsilon_2}{k_2}-\frac{k_2\epsilon_3}{k_0\epsilon_2}\right)\sin(k_2d)\cos(k_1L)+\left.\left(\frac{k_1k_3\epsilon_2}{k_0k_2\epsilon_1}-\frac{k_2\epsilon_1\epsilon_3}{k_1\epsilon_2}\right)\sin(k_1L)\sin(k_2d)\right]\exp[ik_0(L+d)]\ , \tag{2.31a}$$

where in Eq. (2.31a), k_0 is calculated as stated just after Eq. (2.30), while for $i=1$, 2, or 3,

$$k_i=\left(\frac{\omega^2}{c^2}\epsilon_i-Q_{\parallel}^2\right)^{1/2}\ ,\quad \mathrm{Im}(k_i)<0\ . \tag{2.31b}$$

If all the dielectric constants $\epsilon_i(\omega)$ are presumed real (and possibly negative for the two metallic constituents), then $D(Q_{\parallel},\omega)$ has poles at the surface polariton wave vectors for the structure, when $D(Q_{\parallel},\omega)$ is considered as a function of wave vector for fixed frequency. If one or more of the dielectric constants has nonzero imaginary part, then the pole in $D(Q_{\parallel},\omega)$ shifts off the real axis of the $Q_{\parallel}$ plane; the inverse of the imaginary part of $Q_{\parallel}$ at the pole gives the mean free path of the mode, calculated for the structure in Fig. 1 with $\zeta(\vec{x}_{\parallel})$ set to zero. We shall see that in the present analysis, the mean free path of the surface polariton emerges as an important parameter that controls the efficiency of the emission process. Since the presence of surface roughness will also shorten the mean free path, the inverse of the imaginary part of $Q_{\parallel}$ at the pole of $D(Q_{\parallel},\omega)$ provides an upper bound on the mean free path appropriate to a surface polariton on the actual roughened junction.

The quantities $r_\alpha(k_{\parallel}^{(0)},\omega)$ are given by

$$r_\alpha(k_{\parallel}^{(0)},\omega)=\frac{n_\alpha(k_{\parallel}^{(0)},\omega)}{d_\alpha(k_{\parallel}^{(0)},\omega)}\ , \tag{2.32}$$

where $d_x(k_{\parallel}^{(0)},\omega)$ and $d_z(k_{\parallel}^{(0)},\omega)$ are both given by the right-hand side of Eq. (2.31a) but with k_0 replaced by $\omega\cos\theta_0/c$, and the other k_i replaced by

$$k_i=\left(\epsilon_i(\omega)\frac{\omega^2}{c^2}-k_{\parallel}^{(0)2}\right)^{1/2}\equiv\frac{\omega}{c}[\epsilon_i(\omega)-\sin^2\theta_0]^{1/2}\ ,\quad \mathrm{Im}(k_i)<0\ . \tag{2.33}$$

We also have

$$d_y(k_{\parallel}^{(0)},\omega)=\left(1-\frac{k_3}{k_0}\right)\cos(k_1L)\cos(k_2d)+i\left(\frac{k_3}{k_1}-\frac{k_1}{k_0}\right)\cos(k_2d)\sin(k_1L)+i\left(\frac{k_3}{k_2}-\frac{k_2}{k_0}\right)\cos(k_1L)\sin(k_2d)$$
$$+\left(\frac{k_1k_3}{k_0k_2}-\frac{k_2}{k_1}\right)\sin(k_2d)\sin(k_1L)\ , \tag{2.34a}$$

$$n_x(k_{\parallel}^{(0)},\omega)=\frac{k_3}{k_0}\cos(k_1L)\cos(k_2d)+i\frac{k_1\epsilon_3}{k_0\epsilon_1}\cos(k_2d)\sin(k_1L)+i\frac{k_2\epsilon_3}{k_0\epsilon_2}\sin(k_2d)\cos(k_1L)$$
$$-\frac{k_1k_3\epsilon_2}{k_0k_2\epsilon_1}\sin(k_2d)\sin(k_1L)\ , \tag{2.34b}$$

$$n_z(k_{\parallel}^{(0)},\omega)=\epsilon_3\cos(k_2d)\cos(k_1L)+i\frac{\epsilon_1k_3}{k_1}\cos(k_2d)\sin(k_1L)+i\frac{k_3\epsilon_2}{k_2}\sin(k_2d)\cos(k_1L)$$
$$-\frac{\epsilon_1k_2\epsilon_3}{k_1\epsilon_2}\sin(k_2d)\sin(k_1L)\ , \tag{2.34c}$$

and finally

$$n_y(k_{\parallel}^{(0)},\omega)=\cos(k_1L)\cos(k_2d)+i\frac{k_3}{k_1}\cos(k_2d)\sin(k_1L)+i\frac{k_3}{k_2}\cos(k_1L)\sin(k_2d)-\frac{k_2}{k_1}\sin(k_1L)\sin(k_2d)\ . \tag{2.34d}$$

In Eqs. (2.34), we have $k_0 = +\omega\cos\theta_0/c$, and the remaining k_i are calculated through use of the prescription in Eq. (2.33).

The expression in Eq. (2.30) provides a description of the roughness-induced emission from the junction structure, in the limit of small amplitude of surface roughness. The terms in $r_x(k_\parallel^{(0)}, \omega)$ and $r_z(k_\parallel^{(0)}, \omega)$ describe emission of p-polarized radiation, while that in $r_y(k_\parallel^{(0)}, \omega)$ describes emission by s-polarized radiation.

We still have the task of modeling the current fluctuations ahead of us. However, before we turn to this we introduce a number of approximations into Eq. (2.30) which simplify it very considerably and which also introduce little quantitative error.

We shall be interested in the emission of radiation at near infrared and visible frequencies. Thus, the ratio ω/c and also $k_\parallel^{(0)}$ will assume values at most the order of $10^5\,\mathrm{cm}^{-1}$. The most important values of $Q_\parallel$ in the integration on $Q_\parallel$ with the wave vector of the surface polaritons of the structure. We shall see that for frequencies in the range of 1 to 3 eV, for the surface polaritons excited the current fluctuations, we shall have $Q_\parallel \sim 10^6\,\mathrm{cm}^{-1}$. Hence $Q_\parallel >> \omega/c$, and we may replace $|\zeta(\vec{k}_\parallel^{(0)} - \hat{x}Q_\parallel)|^2$ by simply $|\zeta(Q_\parallel)|^2$. Also we may ignore ω/c in the expression for $k_0(Q_\parallel, \omega)$ to obtain $k_0(Q_\parallel, \omega) \cong +iQ_\parallel$, and a similar approximation in the wave vectors k_i in Eq. (2.31b) gives $k_1 \cong k_2 \cong k_3 = -iQ_\parallel$. In the derivation presented here, until now the influence of retardation on the electromagnetic field has been included fully; indeed, we must include retardation to obtain a description of the radiation emitted into the vacuum above the junction. These last approximations are equivalent to the neglect of the influence of retardation in the surface polaritons excited by the fluctuations in the tunneling current, which subsequently radiate as a consequence of the roughness on the outer surface.

After the above assumptions are introduced, the integration on ϕ_0 may be performed. We conclude with one final approximation. This is that all fluctuations in the current density are in the direction perpendicular to the oxide barrier. We invoke this by setting $\mathcal{J}_{xx}$, $\mathcal{J}_{xz}$, and $\mathcal{J}_{zx}$ to zero, and retaining only $\mathcal{J}_{zz}$. This approximation is clearly a sound one in the neighborhood of the oxide barrier, where the tunnel current flows normal to the oxide-metal interfaces. It may be less valid far from the interfaces, but we know of no simple scheme for describing the spatial orientation of the current fluctuations in an actual junction. We do not believe the neglect of the possible presence of nonzero contributions to $\mathcal{J}_{xx}$, $\mathcal{J}_{xz}$, and $\mathcal{J}_{zx}$ has any serious consequence, save in some uncertainty in the numerical value of the quantum efficiency we calculate. For example, after the simplifications outlined in the preceding paragraph are introduced, the angular distribution of the emitted radiation is left completely unaffected by this approximation.

For the frequency and angular distribution of the emitted radiation, we now have an expression very much simpler than the full form in Eq. (2.30):

$$\frac{d^3W}{d\Omega\, d\omega\, dt} = \frac{8\omega^2|\epsilon_1(\omega)-1|^2}{c^3}\left(|r_x(k_\parallel^{(0)},\omega)|^2\cos^2\theta_0 + 2\frac{|r_z(k_\parallel^{(0)},\omega)|^2}{|\epsilon_1(\omega)|^2}\sin^2\theta_0 + |r_y(k_\parallel^{(0)},\omega)|^2\right)$$
$$\times\int_0^\infty \frac{dQ_\parallel Q_\parallel^3|\zeta(Q_\parallel)|^2}{|D_0(Q_\parallel,\omega)|^2}\exp[-2Q_\parallel(L+d)]\int dz\,dz'\,E_z^<(Q_\parallel\omega|z)^*E_z^<(Q_\parallel\omega|z')\mathcal{J}_{zz}(Q_\parallel\omega|zz') \quad . \tag{2.35}$$

Here $D_0(Q_\parallel, \omega)$ is $D(Q_\parallel, \omega)$ calculated with the approximation $Q_\parallel >> \omega/c$ introduced. This gives

$$D_0(Q_\parallel,\omega) = (\epsilon_1+1)\left(\frac{\epsilon_2}{\epsilon_1}+1\right)\left(\frac{\epsilon_3}{\epsilon_2}+1\right) + (\epsilon_1+1)\left(\frac{\epsilon_2}{\epsilon_1}-1\right)\left(\frac{\epsilon_3}{\epsilon_2}-1\right)e^{-2Q_\parallel d}$$
$$+(\epsilon_1-1)\left(\frac{\epsilon_2}{\epsilon_1}-1\right)\left(\frac{\epsilon_3}{\epsilon_2}+1\right)e^{-2Q_\parallel L} + (\epsilon_1-1)\left(\frac{\epsilon_2}{\epsilon_1}+1\right)\left(\frac{\epsilon_3}{\epsilon_2}-1\right)e^{-2Q_\parallel(L+d)} \quad , \tag{2.36}$$

and at the same level of approximation, for $z < L + d$ we have

$$E_z^<(Q_\parallel\omega|z) = \begin{cases} D_+^{(\parallel)}e^{+Q_\parallel z} + D_-^{(\parallel)}e^{-Q_\parallel z}, & d < z < d+L \quad , \\ C_+^{(\parallel)}e^{+Q_\parallel z} + C_-^{(\parallel)}e^{-Q_\parallel z}, & 0 < z < d \quad , \\ e^{+Q_\parallel z}, & -\infty < z < 0 \quad , \end{cases} \tag{2.37}$$

where, with $\sigma = +1$ or -1,

$$D_\sigma^{(\parallel)} = \tfrac{1}{2}e^{-\sigma Q_\parallel d}\left[\left(\frac{\epsilon_3}{\epsilon_1}+\sigma\right)\cosh(Q_\parallel d) + \left(\frac{\epsilon_2}{\epsilon_1}+\sigma\frac{\epsilon_3}{\epsilon_2}\right)\sinh(Q_\parallel d)\right] \tag{2.38a}$$

and

$$C_{\sigma}^{(\mathrm{II})} = \frac{1}{2}\left[\frac{\epsilon_3}{\epsilon_2} + \sigma\right] . \tag{2.38b}$$

At this point, we address our final task in the description of the roughness induced radiation. This is the construction of a model of the frequency spectrum and spatial correlations in the current-density fluctuations. Here we resort to a semiphenomenological model we believe quite reasonable on physical grounds. We shall see that some details of the model influence the radiation spectrum we calculate only modestly.

Through use of a simple version of the tunneling Hamiltonian formalism, Scalapino and collaborators show that the power spectrum[6] $\langle I_{\omega}^2 \rangle$ of the current fluctuations in the junction is given by

$$\langle I_{\omega}^2 \rangle = eI_0(1 - \hbar\omega/eV_0), \quad \hbar\omega < eV_0 , \tag{2.39}$$

with $\langle I_{\omega}^2 \rangle$ zero for $\hbar\omega > eV_0$ and I_0 the dc current which flows in response to the dc voltage V_0. If $I(t)$ is the instantaneous current which flows at time t, and $\delta I(t) = I(t) - I_0$, then $\langle I_{\omega}^2 \rangle$ is the Fourier transform of the correlation function $\langle \delta I(t) \delta I(0) \rangle$.

We proceed by presuming that at each point in space, the current fluctuations have the frequency spectrum given in Eq. (2.39) so that

$$\langle J_z(\vec{x}, \omega) J_z(\vec{x}', \omega) \rangle = eI_0 G(\vec{x}, \vec{x}')(1 - \hbar\omega/eV_0) , \tag{2.40}$$

where $G(\vec{x}, \vec{x}')$ will be a phenomenological form. This function $G(\vec{x}, \vec{x}')$ has the dimensions of $(\text{area})^{-2}$ and from physical considerations must be inversely proportional to the area of the junction, since then $\langle |J_z(x, \omega)|^2 \rangle$ will depend on the current density $J_0 = I_0/A$ carried by the junction and not its geometry. We shall introduce a transverse correlation length ξ_0 that characterizes the spatial correlations present in the current fluctuations, in the plane parallel to the junction. We then write $G(\vec{x}, \vec{x}') = f(\vec{x}, \vec{x}')/\pi\xi_0^2 A$ where $f(\vec{x}, \vec{x}')$ is dimensionless and equal to unity when $\vec{x}' = \vec{x}$. If we suppose that

$$f(\vec{x}, \vec{x}') = \exp(-1/\xi_0 |\vec{x} - \vec{x}'|)\Delta(z,z')$$

with $\Delta(z,z)$ equal to unity, then for $\mathcal{J}_{zz}(Q_{\parallel}\omega|zz')$ we have the phenomenological form, for $\hbar\omega < eV_0$

$$\mathcal{J}_{zz}(Q_{\parallel}\omega|zz') = \frac{eI_0(1 - \hbar\omega/eV_0)}{2\pi^2 A} \frac{\Delta(z,z')}{(1 + Q_{\parallel}^2 \xi_0^2)^{3/2}} . \tag{2.41}$$

Since we have introduced the correlation length ξ_0 in a phenomenological fashion, we have no precise manner of relating this quantity to the properties of the electrons in the junction. An upper bound on ξ_0 is surely the mean free path of the electrons in the junction. This is likely quite small for the thin films employed in the tunnel junction structures utilized so far, which are polycrystalline in nature. We would be surprised if the mean free path is longer than 100 or 200 Å in these films. Scalapino and Rendell[12] argue that the current fluctuations have the character of shot noise, and ξ_0 should be very much shorter than the electron mean free path. This suggests ξ_0 is the order of the Fermi wavelength, a length much smaller than the mean free path. The important point to note from Eq. (2.41) is that as long as ξ_0^{-1} is larger than the wave vector $Q_{\parallel}$ of the surface polariton created by the electron as it tunnels through the junction, the limit $Q_{\parallel}\xi_0 \ll 1$ may be taken in Eq. (2.41) and ξ_0 drops out of the problem. Either choice of ξ_0, the mean free path or the Fermi wavelength, takes us into this limit, unless the electron mean free path becomes the order of a few hundred angstroms.

While the limit $Q_{\parallel}\xi_0 \ll 1$ may well be appropriate to the structures examined to date, we believe it important to note that the spectrum of radiation emitted by the junction can in principle be influenced importantly by spatial correlations in the tunnel current fluctuations. If $Q_{\parallel}\xi_0 \ll 1$, the surface polariton sees the current fluctuations as a superposition of uncorrelated array of fluctuating current columns of diameter small compared to the wavelength of the surface wave, and the probability of exciting the surface polariton depends only on the total number of electrons which contribute to the current fluctuation (this is I_0/eA) and not on the details of their spatial distribution; each tunneling electron can excite a surface polariton independently of the others. If $Q_{\parallel}\xi_0 \gg 1$, correlation between electrons becomes important, the current fluctuations have a spatial extent large compared to the surface polariton of interest, and the excitation efficiency falls off. Equation (2.41) provides a description of the influence of these correlations that is phenomenological, but physically reasonable.

The result in Eq. (2.35) supplemented by the description of the current fluctuations in Eq. (2.41) is the basis for the calculations of the roughness-induced radiation patterns described in Sec. III. We must also model $\Delta(z,z')$. Two choices of this function will be examined in Sec. III.

In Sec. I, we remarked that we have also calculated the frequency spectrum and angular distribution of radiation emitted by the tunneling current fluctuations for the case where all surfaces are presumed perfectly smooth. This radiation has its origin in direct coupling of the current fluctuations to the radiation field outside the junction. We conclude this section by briefly summarizing a derivation of the contribution to the radiation from this source. The approach involves precisely the same ingredients that led us to Eq. (2.35), so we provide only a brief summary of the derivation.

One begins with Eq. (2.2), but for the electromagnetic Green's-function array $D_{\mu\lambda}(\vec{x}\vec{x}';\omega)$ one uses

that appropriate to the structure in Fig. 1 with $\zeta(\vec{x}_{\parallel}) \equiv 0$ rather than the contribution first order in the roughness displayed in Eq. (2.24). Once this is done, the derivation then proceeds in parallel with that given above. In the end, for the power per unit solid angle, per unit frequency interval $d^{3(0)}W^{(0)}/d\Omega\, d\omega\, dt$ we find

$$\frac{d^3W^{(0)}}{d\Omega\, d\omega\, dt} = \frac{2\pi A\,\omega^2}{c^3}\frac{\sin^2\theta_0}{|D(k_{\parallel},\omega)|^2} \times \int dz\, dz'\, E_z^{<}(k_{\parallel}\omega|z) \times E_z^{<}(k_{\parallel}\omega|z')^{*}\mathcal{J}_{zz}(k_{\parallel}\omega|z'z) \quad , \quad (2.42)$$

where A is the area of the junction,[13] and

$$D(k_{\parallel},\omega) = \left(\epsilon_3 - \frac{k_3}{k_0}\right)\cos(k_2 d)\cos(k_1 L) + i\left(\frac{\epsilon_1 k_3}{k_1} - \frac{k_1\epsilon_3}{k_0\epsilon_1}\right)\cos(k_2 d)\sin(k_1 L) + i\left(\frac{k_3\epsilon_2}{k_2} - \frac{k_2\epsilon_3}{k_0\epsilon_2}\right)\sin(k_2 d)\cos(k_1 L) + \sin(k_2 d)\sin(k_1 L)\left(\frac{k_1 k_3\epsilon_2}{k_0 k_2\epsilon_1} - \frac{k_2\epsilon_1\epsilon_3}{k_1\epsilon_2}\right) . \quad (2.43)$$

In all quantities which appear in Eqs. (2.42) and (2.43), the quantity $k_{\parallel} = (\omega/c)\sin\theta_0$. Thus, to calculate $E_z^{<}(k_{\parallel}\omega|z)$ and $D(k_{\parallel},\omega)$ one takes $k_0 = \omega\cos\theta_0/c$ as in Eq. (2.10b), while k_1, k_2, and k_3 are computed from the prescription in Eq. (2.33).

This completes the derivation of the basic expressions that will form the basis of the numerical studies presented in Sec. III, and which lead us to the conclusions set forth in Sec. I. The formulas presented here contain a complete description of radiation emitted by fluctuations in the tunneling current, including the polarization properties and angular distribution of the emitted radiation.[14] In Eq. (2.42), we have the spectrum of radiation emitted by current fluctuations in a structure of the form illustrated in Fig. 1 with perfectly smooth surfaces, while Eq. (2.35) describes the radiation that results from roughness on the surface, in the limit that the roughness may be treated by perturbation theory.

III. DISCUSSION OF NUMERICAL CALCULATIONS

In this section, we discuss the results of our numerical studies of the frequency spectrum and polarization properties of light emitted by the junctions. We have carried out studies for an aluminum substrate, upon which an oxide film has been deposited followed by an overlayer of either Au or Ag.

It is important to understand the dispersion relation for surface polaritons in these structures. We have calculated the real and imaginary parts of the wave vector $Q_{\parallel}$ for the modes by finding the complex roots of the function $D_0(Q_{\parallel},\omega)$ in Eq. (2.36). To do this, the dielectric constant ϵ_2 of the oxide layer was taken equal to 3.0, following Davis, while for ϵ_1 and ϵ_3 we employed experimental values of the complex dielectric constant of the bulk materials from which the substrate and the outer film are constructed. Because the imaginary part of ϵ_1 and ϵ_3 are nonzero, energy is dissipated within the metals when the surface polariton is excited, and its mean free path is thus finite. The distance required for the electric field *amplitude* to decay to e^{-1} of its initial value is given by the inverse of the imaginary part of $Q_{\parallel}$.

For selected values of L and d, we display the real and imaginary parts of $Q_{\parallel}$ in Fig. 2. Only the lower branch of the surface polariton dispersion relation will enter our discussion, and we display only this branch. It is important to note two features of the curves. First, for the case where Au is superimposed over the oxide, the surface polariton dispersion curve approaches the asymptotic frequency of roughly 2.2 eV, and there are no well-defined modes of the structure above this frequency (in the visible). For a Ag film as the upper layer, the asymptotic frequency is 3.5 eV, a value substantially higher than Au. This will lead us to predict very different spectra for tunnel junctions made from Ag, and those made from Au. Second, the imaginary part of $Q_{\parallel}$ is about ten times smaller than the real part, for the frequencies explored in the figure. Thus, the surface polaritons are only modestly damped by the dissipation in the substrate.

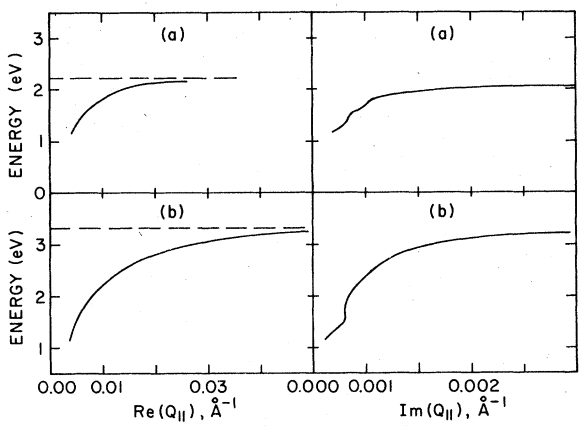

FIG. 2. We present here the real and imaginary parts for the wave vector $Q_{\parallel}$ of surface polaritons that propagate within the tunnel junction structure illustrated in Fig. 1. The calculations are presented for (a) Au deposited on Al, with a 30-Å oxide layer, and (b) Ag deposited on Al, with a 30-Å oxide layer.

In Fig. 2, one sees that as $Q_\parallel \to 0$, the frequency of the surface polariton vanishes. Our model, with the upper film taken to have finite thickness L, produces a behavior as $Q_\parallel \to 0$ rather different than Davis found upon taking L infinite. This is difficult to appreciate from the numerical calculations, but may be illustrated as follows. Suppose the outer film is presumed to have a real dielectric constant $\epsilon_1(\omega) = \epsilon_1^{(\infty)} - \omega_{p_1}^2/\omega^2$ while the substrate has $\epsilon_3(\omega) = \epsilon_3^{(\infty)} - \omega_{p_3}^2/\omega^2$. For such a model, as $\omega \to 0$ one can extract an analytic expression for the dispersion curve. For the case $L \to \infty$, as $Q_\parallel \to 0$, in the regime $Q_\parallel d \ll 1$ one has

$$\omega(Q_\parallel) = \frac{\omega_{p_1}\omega_{p_2}}{[\epsilon_2(\omega_{p_1}^2 + \omega_{p_3}^2)]^{1/2}} (Q_\parallel d)^{1/2} \quad . \tag{3.1}$$

From this expression, it is evident that the low-frequency branch owes its existence to the presence of the oxide layer.

With L finite, a different behavior follows as $Q_\parallel \to 0$. If we have $Q_\parallel d \ll 1$, and $\omega^2 < \omega_{p_1}^2$, $\omega^2 < \omega_{p_3}^2$ in the model used to obtain Eq. (3.1), then from Eq. (2.36), we find Eq. (3.1) is modified to read

$$\omega(Q_\parallel) = \frac{\omega_{p_1}\omega_{p_3}}{[\epsilon_2(\omega_{p_1}^2 + \omega_{p_3}^2)]^{1/2}} (Q_\parallel d \tanh Q_\parallel L)^{1/2} \tag{3.2}$$

so when $Q_\parallel L \ll 1$, we find $\omega(Q_\parallel)$ varies linearly with $Q_\parallel$ rather than as $Q_\parallel^{1/2}$. This behavior is illustrated in Fig. 3.

From Fig. 2, as we have remarked, one sees that the imaginary part of $Q_\parallel$ is small compared to the real part. This means that in the complex $Q_\parallel$ plane, $D_0(Q_\parallel, \omega)$ has a pole near the real axis. This suggests that the integral on $Q_\parallel$ in Eq. (2.35) may be evaluated by an approximation that isolates only the contribution from the surface polariton pole. If we assume ω lies below the cutoff frequency for the surface polariton dispersion curves in Fig. 2, then we proceed as follows. In all quantities inside the integrand of Eq. (2.35), save for $|D_0(Q_\parallel, \omega)|^2$ which varies rapidly as $Q_\parallel$ passes through the surface polariton resonance, we replace $Q_\parallel$ by the real part $Q_\parallel^{(R)}(\omega)$ of the wave vector of the surface polariton of frequency ω. Then for $D_0(Q_\parallel, \omega)$, for fixed ω, we use a Taylor-series expansion about the surface polariton pole. We thus write

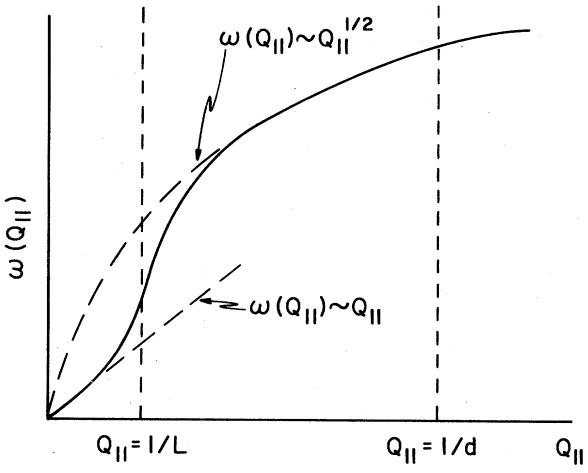

FIG. 3. Schematic diagram of the surface polariton dispersion relation, to illustrate the effect of the finite thickness L of the upper film. The sketch applies to the regime $Q_\parallel d \ll 1$, but $Q_\parallel L$ arbitrary.

$$D_0(Q_\parallel, \omega) = D_0'(\omega)[Q_\parallel - Q_\parallel^{(R)}(\omega) - iQ_\parallel^{(I)}(\omega)] \quad , \tag{3.3}$$

where $D_0'(\omega) = (\partial D_0/\partial Q_\parallel)|_{Q_\parallel = Q_\parallel^{(R)}(\omega)}$. The integral on $Q_\parallel$ that remains is elementary, and we replace Eq. (2.35) by

$$\frac{d^3W}{d\Omega\, d\omega\, dt} = \frac{8\pi\omega^2|\epsilon_1(\omega)-1|^2}{c^3 Q_\parallel^{(I)}(\omega)} \left(|r_x(k_\parallel^{(0)}, \omega)|^2 \cos^2\theta_0 + 2\frac{|r_2(k_\parallel^{(0)}, \omega)|^2}{|\epsilon_1(\omega)|^2} \sin^2\theta_0 + |r_y(k_\parallel^{(0)}, \omega)|^2 \right) \cdot$$
$$\times \frac{Q_\parallel^{(R)}(\omega)^3 |\zeta(Q_\parallel^{(R)}(\omega))|^2}{|D_0'(\omega)|^2} \exp[-2Q_\parallel^{(R)}(\omega)(L+d)]$$
$$\times \int dz\, dz'\, E_z^<(Q_\parallel^{(R)}(\omega)\omega|z)^* E_z^<(Q_\parallel^{(R)}(\omega)\omega|z') \mathcal{J}_{zz}(Q_\parallel^{(R)}(\omega), \omega|zz') \quad . \tag{3.4}$$

In the numerical calculations below, we have used the result in Eq. (3.4) principally. Its accuracy has been checked by full numerical evaluation of the integral in Eq. (2.35), and we find Eq. (3.4) works very well.

It is important to note that the intensity of radiation is inversely proportional to $Q_\parallel^{(I)}(\omega)$, which is itself the inverse of the mean free path $l(\omega)$ of the surface polariton of frequency ω. Thus, the intensity of the radiation is, among other things, directly proportional to the mean free path.

Our present theory, which calculates the emission intensity only to lowest order in the roughness amplitude, instructs us to calculate the mean free path

from study of the complex roots of $D_0(Q_{\parallel}, \omega)$ in Eq. (2.36). The mean free path is thus finite because of dissipation of energy within the various components of the structure.

But the surface is also rough, and the presence of roughness will shorten the mean free path of the surface polariton.[4] The mean path calculated as just outlined is thus an upper bound to the value appropriate to an actual device with roughened surface. Actually, $l(\omega)$ should be chosen to be the mean free path of the surface polariton on the actual structure. Then as the amplitude of the roughness is increased, $|\zeta(Q_{\parallel}^{(R)}(\omega))|^2$ increases with the square of the amplitude, but at the same time the mean free path shortens. In fact, the simplest prescription for calculating $l(\omega)$ in the presence of roughness shows that as the amplitude of the roughness increases, the intensity of the emitted radiation *saturates* at a value independent of the amplitude of the roughness. One sees this as follows. Let $l_0(\omega)$ be the mean free path calculated for the structure with smooth surfaces, i.e., $l_0(\omega)$ has its origin in energy dissipation in the substrate. Then, if the amplitude of the roughness is small, we can follow the procedures of Ref. 4 and calculate an additional contribution to the attenuation rate of the wave from surface roughness. Call this contribution to the imaginary part of $Q_{\parallel}$ $l_{\delta}^{-1}(\omega)$. Then in the presence of both mechanisms, the mean free path is calculated by adding the scattering rates

$$\frac{1}{l(\omega)} = \frac{1}{l_0(\omega)} + \frac{1}{l_{\delta}(\omega)} \quad . \tag{3.5}$$

In perturbation theory, $[l_{\delta}(\omega)]^{-1}$ is proportional to δ^2, the square of the roughness amplitude. Thus, if δ^2 is so large that $l_{\delta}(\omega) \ll l_0(\omega)$, then the intensity of the emitted radiation is proportional to $|\zeta(Q_{\parallel}^{(R)}(\omega))|^2 l_{\delta}(\omega)$ and is independent of δ^2. In words, as δ^2 increases, the surface polariton decouples from the surface more efficiently [$|\zeta(Q_{\parallel}^{(R)}(\omega))|^2$ increases], but the surface polariton is on the surface and capable of radiating for only a very short distance [$l(\omega)$ decreases]. In the above simple picture, the two effects compensate when the amplitude of the roughness gets large. We believe the above prescription may be justified by describing the propagation of the surface polariton on the roughened surface by the averaged Green's functions introduced by Maradudin and Zierau.[15]

Lambe and McCarthy[3] have observed that as the roughness amplitude increases, for tunnel junctions grown on CaF_2 substrates, the intensity of emitted radiation indeed saturates. These authors suggested that the reason for this was that the surface polariton becomes heavily damped on the rougher surfaces. The argument above is consistent with this viewpoint, and shows in concrete terms how such a feature emerges from the theory. We also have an explicit criterion for the onset of saturation, in a given frequency range, namely that $l_{\delta}(\omega) \cong l_0(\omega)$. All calculations reported here use $l_0(\omega)$ for the mean free path and ignore the influence of roughness on it; we have underway a detailed study of the influence of roughness on the mean free path of surface polaritons in these structures. This analysis, and a quantitative study of the mechanism for saturation proposed above will be presented in a subsequent publication.

We now turn to a description of our calculations of the frequency spectrum and angular distribution of the emitted radiation. For this purpose, we use Eq. (3.4). We have checked the accuracy of the "pole approximation" upon which Eq. (3.4) is based by direct numerical integration of the full form in Eq. (2.35), and we find the pole approximation provides less than ten percent error for all calculations we report. Note that the *angular* distribution of the radiation is controlled by only the prefactor in Eq. (3.4) which involves the quantities $|r_x(k_{\parallel}^{(0)}, \omega)|^2$, $|r_y(k_{\parallel}^{(0)}, \omega)|^2$, and $|r_z(k_{\parallel}^{(0)}, \omega)|^2$.

We have formed from the expression in Eq. (3.4) a dimensionless quantity which describes the frequency spectrum, and plays the role of a frequency and angle-dependent quantum efficiency. Note that the number of photons per unit time, per unit solid angle is given by

$$\frac{dN_P}{d\Omega\, dt} = \int_0^{\omega_c} \frac{d\omega}{\hbar\omega} \frac{d^3W}{d\Omega\, d\omega\, dt} \quad , \tag{3.6}$$

where $\omega_c = eV_0/\hbar$ is the maximum photon frequency. The number of electrons per unit time that pass through the junction is I_0/e. Thus, we form the quantity

$$\frac{dQ(\omega)}{d\Omega} = \frac{e^2 V_0}{\hbar^2 \omega I_0} \frac{d^3W}{d\Omega\, d\omega\, dt} \quad , \tag{3.7}$$

which is dimensionless, and the integral $\int_0^{\omega_c} (d\omega/\omega_c)(dQ/d\Omega)$ is the probability per unit solid angle that an electron that has tunneled through the barrier emits a photon in a given direction.

Finally, in all the calculations we report, the function $\Delta(z,z')$ which appears in Eq. (2.41) has been set equal to unity. This means we model the current fluctuations as vertical in direction, extending throughout the tunnel junction structure. We find the choice of $\Delta(z,z')$ has little influence on the dependence of $dQ/d\Omega$ on frequency and little influence on the angular distribution. However, the magnitude is affected by this choice. For example, if we choose $\Delta(z,z')$ nonzero only within the oxide barrier to mimic the picture employed by Scalapino *et al.*, the values of $dQ/d\Omega$ are found to be smaller than those we report here by a factor of 300 to 1000, depending on the remaining parameters. It seems to us that the resulting values of $dQ/d\Omega$ are then much smaller than those reported,[1] so we suggest that the

surface polariton is driven by fluctuations that extend throughout the structure; our picture of the spatial distribution of the fluctuations is only schematic, but we find values of $dQ/d\Omega$ comparable to or possibly a bit larger than those reported.

In Fig. 4(a), we present values of $dQ/d\Omega$ calculated for emission from a roughened 200-Å film of Ag separated from Al by a 30-Å oxide layer. The emission angle is 45° off the normal to the film surface. The root-mean-square amplitude of the roughness δ has been chosen equal to 35 Å, a value we believe comparable to that on the samples used by Lambe and McCarthy, while $|\zeta(Q_{\parallel})|^2$ is taken to have the Gaussian form used in earlier work

$$|\zeta(Q_{\parallel})|^2 = \pi A a^2 \delta^2 \exp(-\tfrac{1}{4} a^2 Q_{\parallel}^2) \ , \qquad (3.8)$$

where a, the transverse correlation length, provides a rough measure of the separation between adjacent peaks on the rough surface.

Several features in Fig. 4(a) are worth comment. Recall that the maximum surface polariton frequency for the structure is 3.25 eV [Fig. 2(b)]. Curve number (1) is calculated with the value of the correlation length chosen to be 100 Å, a value short enough so the frequency spectrum is not influenced by ξ_0. The transverse correlation length a is chosen to be 500 Å, a value comparable to that reported in the optical literature for films grown on CaF_2 substrates.[8] We see the frequency spectrum "cuts off" well below 3.25 eV, since the transverse correlation length is so long, the large wave-vector surface polaritons near 3.25 eV cannot decouple from the surface and radiate. Curve number (2) is calculated with the same value of a, but now with ξ_0 chosen to be 500 Å rather than 100 Å. The curve on the figure is the emission intensity multiplied by a factor of 10. Thus, for large ξ_0, the emission is supressed throughout the near infrared and visible. The reason is that when the correlation length is this long, the current fluctuations with high spatial correlation are unable to excite the surface polaritons.

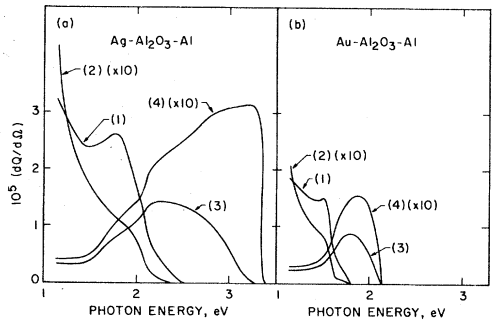

FIG. 4. Roughness induced emission spectrum, at an angle of 45° with respect to the normal for a model tunnel junction structure with a 30-Å oxide layer and with (a) 200-Å outer film of Ag, and (b) 200-Å outer film of Au. For each figure, we calculate the quantity $dQ/d\Omega$ defined in Eq. (3.7), and we have chosen $\delta = 35$ Å. In each part of the Figure, curve (1) is calculated for $a = 400$ Å and $\xi_0 = 100$ Å, curve (2) for $a = 400$ Å, and $\xi_0 = 500$ Å, curve (3) for $a = 100$ Å and $\xi_0 = 100$ Å, and curve (4) for $a = 35$ Å and $\xi_0 = 100$ Å. For clarity, in both parts of the figure, curve (2) and curve (4) are multiplied by a factor of 10.

Curve (3) has $\xi_0 = 100$ Å, value small enough that the spectrum is not influenced by this parameter. Here the transverse correlation length is 100 Å, and we see emission that extends up to the surface polariton cutoff frequency of 3.25 eV; recall that in Fig. 4(a), the voltage is 4 volts, so we see here the explicit dependence of the emission spectrum on the surface polariton dispersion curve.

Finally, curve (4) is calculated with the transverse correlation length equal to 35 Å, and again $\xi_0 = 100$ Å. We find strong emission in the visible, now with emission in the near infrared weaker than for curve (3). With such a small correlation length, it appears as if the short-wavelength surface polaritons decouple from the surface efficiently, but now the longer wavelength modes radiate more weakly.

In Fig. 4(b), we present a similar series of calculations for a Au overlayer rather than a Ag overlayer, with the same series of parameters.

From the curves in Fig. 4, it is evident that small scale roughness with a transverse correlation length in the range of 50 Å is required to produce strong emission which extends into the visible. As remarked earlier optical studies of films grown on CaF_2 substrates (which produce rough surfaces) suggest the transverse correlation length is the order of 400 Å. With such a correlation length, we cannot account for the presence of emission in the visible, at least by means of the second-order mechanism proposed by Lambe and McCarthy. It is likely that the optical reflectivity is not affected by roughness on the 50-Å length scale. We may envision an undulating random structure, characterized by the long correlation length sensed by the optical studies. Superimposed on this one has fine structures of steps and terraces, characterized by a much shorter characteristic length. Such a picture seems quite a reasonable one, and seems required to explain the emission spectra of the junction structures within our model. We note that in their analysis of radiation by spherical particles placed on the oxide layer, Scalapino *et al.* take the sphere they examine to be $r = 150$ Å, and place it on an oxide layer $d = 20$ Å thick. They argue that the surface polaritons responsible for the radiation are "trapped" in a region of spatial extend $(rd)^{1/2} \approx 65$ Å. Thus, in their picture, the "active" regions on the surface are comparable in spatial extent to the transverse correlation length we require. Thus, while both theories begin from very different starting points, a crude correspondence between them can be established.

For Au, with the short correlation length we choose, Fig. 4(b) shows a peak in our calculated emission spectrum near 1.8 or 1.9 eV, depending on the value chosen for a. This comes from radiation produced by surface polaritons on the "knees" of the dispersion curve, with $Q_{\parallel} \approx 10^6$ cm^{-1}. Here $Q_{\parallel} a \approx 1$, and these modes radiate efficiently for transverse correlations lengths on the 50-Å scale. Scalapino *et al.*[6] also find a peak in the spectral emission at around 1.9 eV, and this feature appears clearly in the data of Hansma and collaborators.[1] By comparing the two theories, we see again a similarity, even though the starting point is very different. The 1.9-eV peak seems likely to appear in the emission spectrum of Au, under a wide variety of conditions.

In Figs. 5(a) and 5(b), we show the angular distribution of emitted radiation from a Ag film and a Au film, calculated for $a = 35$ Å and $\xi_0 = 100$ Å, and for several photon frequencies. In all cases, the emission is most intense along the normal to the film and falls smoothly to zero as the emission angle approaches 90°. The radiation is about an equal admixture of s- and p-polarized radiation. About half comes from the term in $|r_x|^2$, about half from the term in $|r_y|^2$, and the term in $|r_z|^2$ gives a very small contribution.

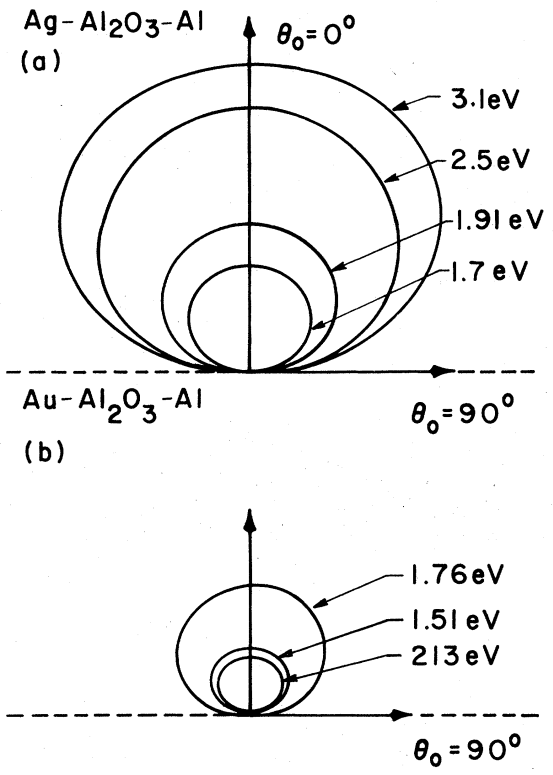

FIG. 5. Angular distribution of radiation from (a) a 200-Å thick Ag film, and (b) a 200-Å thick Au film, for several photon frequencies. In these calculations, we have taken $a = 35$ Å, $\delta = 35$ Å, the voltage $v_0 = 4$ volts, and $\xi_0 = 100$ Å.

Here we have a substantial difference between our calculation, and those of Scalapino *et al.* They find only p-polarized radiation from their spheres, and also they find strongest emission off the normal by about 55°. Thus, the polarization properties and angular distribution of the emitted radiation are very different indeed in the two theories.

Recently Adams, Wyss, and Hansma[1] have measured the polarization properties and angular distribution of radiation from an oxide aluminum film with globules of Au laid on top. They find both s- and p-polarized radiation of roughly equal intensity. The s-polarized radiation has an angular distribution virtually identical to that we calculate and present in Fig. 5(b). The situation is more complex with the p-polarized radiation. First, there is a maximum off the surface normal, in a position quite consistent with expectations from the radiating sphere model. But this model shows the intensity of the p-polarized radiation must vanish along the normal, while the data shows that the p-polarized radiation becomes equal in intensity to the s-polarized radiation along the normal. Our calculation produces precisely this behavior, but to repeat, no maximum off the normal.

The analysis presented by Adams, Wyss, and Hansma[1] suggests the p-polarized radiation may be decomposed into two components. One has angular distribution very similar to that we calculate, and one has distribution in excellent accord with the radiating sphere model. This suggests that the emission observed from this very complex experimental geometry may be thought of as a superposition of radiation from roughly spherical Au particles, and from extended, irregular structures mimiced in some crude sense by our random roughness model.

In Sec. I, we derived expressions for the emission intensity from the roughness-induced radiation, and also from direct coupling of fluctuations in the tunneling current to the transverse radiation field. We conclude by presenting calculations of the intensity and angular distribution of radiation from this source, which operates even when the film surfaces are perfectly smooth. Our motivation for doing this comes from one of the emission spectra in the original paper by Lambe and McCarthy. For one Au film, they show the emission spectrum for a junction biased at 4 volts. The radiation extends right up to 4 volts, even though the cutoff in the surface polariton dispersion curve is around 2.2 eV. It seems difficult to account for this emission on the basis of the second-order mechanism, with the essential role the surface polariton plays.

In Fig. 6(a), for a junction with a Au film biased at 4 volts, we show the frequency spectrum and magnitude of radiation emitted by a structure with perfectly smooth surfaces. The Au film was presumed 200 Å thick. We see the intensity of the emission is quite comparable in magnitude from that calculated from

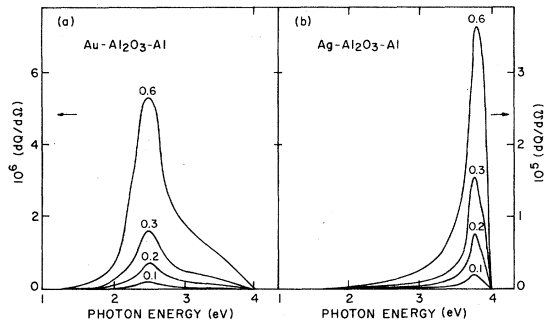

FIG. 6. Frequency spectrum and magnitude of the emission spectrum ($dQ/d\Omega$) for emission from (a) a Au film 200 Å thick with smooth surfaces, and (b) a Ag film with 200 Å thick smooth surfaces. We present spectra calculated for several emission angles. The bias voltage is 4 volts.

the surface polariton induced mechanism. The radiation is most intense at a frequency which is just above the onset of the contribution of interband electronic transitions to ϵ_2 in Au. The long tail that extends up to the 4-volt cutoff bears a resemblence to the spectrum that appears in the paper by Lambe and McCarthy. Figure 6(b) shows a similar calculation for Ag. Here the emission again sets in at a frequency where interband transitions enter ϵ_2; we see the emission for Ag is much stronger than that from Au. We have carried out a calculation for a bias voltage of 6 volts, and we find a peak at around 4 eV followed by a long tail similar to that in Au.

The "smooth surface" emission is purely p polarized; the angular distribution for Au is presented in Fig. 7. The fact that we get zero emission along the normal to the film is a consequence of confining attention only to current fluctuations parallel to the z direction.

By synthesizing the "smooth-surface" emission with that from the surface polariton mediated process, we can produce angular distributions with a striking frequency dependence, for bias voltages which pass through the surface polariton cutoff frequency. We illustrate this in Fig. 8 where the two are superimposed for a particular combination of parameters. A study of the distribution of the radiation in both angle and frequency will thus enable one to sort out the two contributions, at least for tunnel junction structures that mimic our random roughness model.

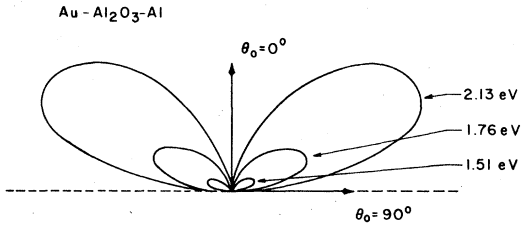

FIG. 7. Angular distribution for several photon frequencies, for emission from a 200-Å Au film with smooth surfaces.

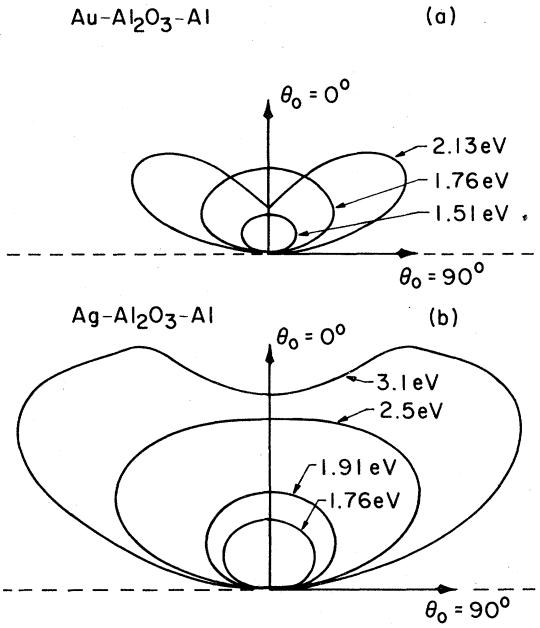

FIG. 8. For $\delta = 35$ Å, and $a = 35$ Å, we synthesize the emission produced by the second-order surface polariton-mediated mechanism, with that from direct coupling of tunnel current fluctuations to the radiation field. We do this for (a) Au and (b) Ag.

Finally, Fig. 9 gives a calculation of the frequency spectrum for emission from Ag, calculated by combining the two contributions as in Fig. 8. The curves resemble the data in the original paper by Lambe and McCarthy.[1]

This summarizes the calculations we have carried out using the theoretical development presented in Sec. II. We presently have under study the influence

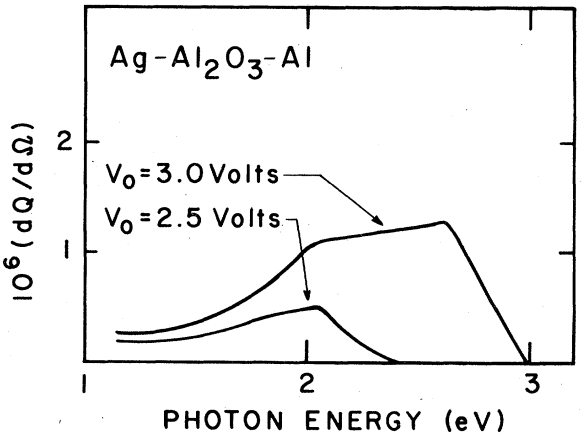

FIG. 9. Frequency spectrum calculated for emission from a Ag film on the oxide, for the parameters used to construct Fig. 8.

of roughness on the mean free path of the surface polariton to see if the mechanism proposed here indeed leads to saturation of the output, for a reasonable choice of parameters. This analysis will be described in a subsequent publication.

ACKNOWLEDGMENTS

We have been greatly stimulated by conversations with Professor D. J. Scalapino, R. Rendell, and Professor P. K. Hansma. We acknowledge support for the research from the Air Force Office of Scientific Research, through Contract No. F49620-78-C-0019 and one of us (B.L.) is partially supported by a fellowship from CNPq (Conselho Nacional de Desenvolvimento Cientifico e Tecnologico, Brazil).

APPENDIX: THE ELECTROMAGNETIC GREEN'S FUNCTIONS FOR THE TUNNEL JUNCTION STRUCTURE

The calculation of the radiation intensity emitted by the junction requires the explicit form of the functions $d_{\mu\lambda}^{(0)}(\vec{Q}_{\parallel}\omega|zz')$ defined in Eq. (2.25) of the present text. For a related geometry, these functions have been derived in the Appendix of an earlier paper on surface roughness.[16] The forms given there are applicable to a variety of planar geometries. Thus, we do not derive the new forms here, but will simply set forth the expressions which must be inserted into the general forms given earlier.

The set of functions $d_{\mu\lambda}^{(0)}(\vec{Q}_{\parallel}\omega|zz')$ may be expressed in terms of a simpler set $g_{\mu\lambda}^{(0)}(Q_{\parallel}\omega|zz')$ by use of the transformation stated in Eq. (A5) of the earlier paper. The nonzero elements of the array $g_{\mu\lambda}^{(0)}(Q_{\parallel}\omega|zz')$ are expressed in terms of certain electromagnetic fields $E_{\alpha}^{<}(Q_{\parallel}\omega|z)$ and $E_{\alpha}^{>}(Q_{\parallel}\omega|z)$ which emerge from the solutions of Maxwell's equation for the structure, with boundary conditions imposed as earlier. We begin by stating the forms of these fields for the present structure. In what follows, k_0 is defined as in Eq. (2.30) of this paper, and for $i=1$, 2, or 3, the quantities k_i are defined as in Eq. (2.31b).

We then have the following expressions for the required field components:

$$E_x^{>}(Q_{\parallel}\omega|z)=\begin{cases}-\dfrac{k_0}{Q_{\parallel}}e^{ik_0z}, & z>L+d\ ,\\ -\dfrac{k_1}{Q_{\parallel}}(A_+^{(\parallel)}e^{ik_1z}-A_-^{(\parallel)}e^{-ik_1z}), & d<z<L+d\ ,\\ -\dfrac{k_2}{Q_{\parallel}}(B_+^{(\parallel)}e^{ik_2z}-B_-^{(\parallel)}e^{-ik_2z}), & 0<z<d\ ,\\ -\dfrac{k_3}{Q_{\parallel}}(T_+^{(\parallel)}e^{ik_3z}-T_-^{(\parallel)}e^{-ik_3z}), & z<0\ ,\end{cases} \tag{A1a}$$

$$E_z^{>}(Q_{\parallel}\omega|z)=\begin{cases}e^{ik_0z}, & z>L+d\ ,\\ A_+^{(\parallel)}e^{ik_1z}+A_-^{(\parallel)}e^{-ik_1z}, & d<z<L+d\ ,\\ B_+^{(\parallel)}e^{ik_2z}+B_-^{(\parallel)}e^{-ik_2z}, & 0<z<d\ ,\\ T_+^{(\parallel)}e^{ik_3z}+T_-^{(\parallel)}e^{-ik_3z}, & z<0\ ,\end{cases} \tag{A1b}$$

where, with $\sigma=+$ or $-$, we have

$$A_{\parallel}^{(\sigma)}=\frac{1}{2}\left(\frac{1}{\epsilon_1}+\sigma\frac{k_0}{k_1}\right)\exp[i(k_0-\sigma k_1)(L+d)]\ , \tag{A2a}$$

$$B_{\parallel}^{(\sigma)}=\tfrac{1}{2}\exp[ik_0(L+d)-i\sigma k_2d]\left[\cos(k_1L)\left(\frac{1}{\epsilon_2}+\sigma\frac{k_0}{k_2}\right)-i\sin(k_1L)\left(\frac{k_0\epsilon_1}{k_1\epsilon_2}+\sigma\frac{k_1}{k_2\epsilon_1}\right)\right]\ , \tag{A2b}$$

and

$$T_{\parallel}^{(\sigma)}=\tfrac{1}{2}e^{ik_0(L+d)}\left[\cos(k_1L)\cos(k_2d)\left(\frac{1}{\epsilon_3}+\sigma\frac{k_0}{k_3}\right)-i\cos(k_1L)\sin(k_2d)\left(\frac{k_0\epsilon_2}{k_2\epsilon_3}+\sigma\frac{k_2}{\epsilon_2k_3}\right)\right.$$
$$\left.-i\sin(k_1L)\cos(k_2d)\left(\frac{k_0\epsilon_1}{k_1\epsilon_3}+\sigma\frac{k_1}{k_3\epsilon_1}\right)-\sin(k_1L)\sin(k_2d)\left(\frac{k_1\epsilon_2}{k_2\epsilon_1\epsilon_3}+\sigma\frac{k_0k_2\epsilon_1}{k_1k_3\epsilon_2}\right)\right]\ . \tag{A2c}$$

Then we also require

$$E_x^<(Q_\parallel\omega|z)=\begin{cases}-\dfrac{k_0}{Q_\parallel}(R_+^{(\parallel)}e^{ik_0z}-R_-^{(\parallel)}e^{-ik_0z}), & z>L+d\ ,\\ -\dfrac{k_1}{Q_\parallel}(D_+^{(\parallel)}e^{ik_1z}-D_-^{(\parallel)}e^{-ik_1z}), & d<z<L+d\ ,\\ -\dfrac{k_2}{Q_\parallel}(C_+^{(\parallel)}e^{ik_2z}-C_-^{(\parallel)}e^{-ik_2z}), & 0<z<d\ ,\\ -\dfrac{k_3}{Q_\parallel}e^{ik_3z}, & z<0\ ,\end{cases} \tag{A3a}$$

and

$$E_z^<(Q_\parallel\omega|z)=\begin{cases}R_+^{(\parallel)}e^{ik_0z}+R_-^{(\parallel)}e^{-ik_0z}, & z>L+d\ ,\\ D_+^{(\parallel)}e^{ik_1z}+D_-^{(\parallel)}e^{-ik_1z}, & d<z<L+d\ ,\\ C_+^{(\parallel)}e^{ik_2z}+C_-^{(\parallel)}e^{-ik_2z}, & 0<z<d\ ,\\ e^{ik_3z}, & z<0\ .\end{cases} \tag{A3b}$$

Here, again with $\sigma=+$ or $-$,

$$R_\sigma^{(\parallel)}=\tfrac{1}{2}e^{-i\sigma k_0(L+d)}\left[\left(\epsilon_3+\sigma\frac{k_3}{k_0}\right)\cos(k_2d)\cos(k_1L)+i\left(\frac{\epsilon_1k_3}{k_1}+\sigma\frac{k_1\epsilon_3}{k_0\epsilon_1}\right)\cos(k_2d)\sin(k_1L)\right.$$
$$\left.+i\left(\frac{k_3\epsilon_2}{k_2}+\sigma\frac{k_2\epsilon_3}{k_0\epsilon_2}\right)\sin(k_2d)\cos(k_1L)-\sin(k_2d)\sin(k_1L)\left(\frac{k_2\epsilon_1\epsilon_3}{k_1\epsilon_2}+\sigma\frac{k_1k_3\epsilon_2}{k_0k_2\epsilon_1}\right)\right]\ , \tag{A4a}$$

$$D_\sigma^{(\parallel)}=\tfrac{1}{2}e^{-i\sigma k_1d}\left[\left(\frac{\epsilon_3}{\epsilon_1}+\sigma\frac{k_3}{k_1}\right)\cos(k_2d)+i\left(\frac{k_3\epsilon_2}{k_2\epsilon_1}+\sigma\frac{k_2\epsilon_3}{k_1\epsilon_2}\right)\sin(k_2d)\right]\ , \tag{A4b}$$

and

$$C_\sigma^{(\parallel)}=\frac{1}{2}\left(\frac{\epsilon_3}{\epsilon_2}+\sigma\frac{k_3}{k_2}\right)\ . \tag{A4c}$$

The four fields above, combined with

$$W_\parallel(Q_\parallel,\omega)=\frac{\omega^2k_0}{ic^2Q_\parallel^2}e^{+ik_0(L+d)}\left[\left(\epsilon_3-\frac{k_3}{k_0}\right)\cos(k_2d)\cos(k_1L)+i\left(\frac{\epsilon_1k_3}{k_1}-\frac{k_1\epsilon_3}{k_0\epsilon_1}\right)\cos(k_2d)\sin(k_1L)\right.$$
$$\left.+\left(\frac{k_3\epsilon_2}{k_0\epsilon_2}-\frac{k_2\epsilon_3}{k_0\epsilon_2}\right)\sin(k_2d)\cos(k_1L)-\sin(k_2d)\sin(k_1L)\left(\frac{k_2\epsilon_1\epsilon_3}{k_1\epsilon_2}-\frac{k_1k_3\epsilon_2}{k_0k_2\epsilon_1}\right)\right] \tag{A5}$$

allow us to construct the elements $g_{xx}^{(0)}$, $g_{xz}^{(0)}$, $g_{zx}^{(0)}$, and $g_{zz}^{(0)}$ of the tensor $g_{\mu\lambda}^{(0)}$. We have only $g_{yy}^{(0)}$ left, since $g_{yz}^{(0)}$ and $g_{zy}^{(0)}$ vanish identically. We can construct $g_{yy}^{(0)}$ from the prescription given earlier,[12] and through use of

$$E_y^>(Q_\parallel\omega|z)=\begin{cases}e^{+ik_0z}\ ,\\ A_+^{(\perp)}e^{ik_1z}+A_-^{(\perp)}e^{-ik_1z}, & d<z<d+L\ ,\\ B_+^{(\perp)}e^{ik_2z}+B_+^{(\perp)}e^{-ik_2z}, & 0<z<d\ ,\\ T_+^{(\perp)}e^{ik_3z}+T_-^{(\perp)}e^{-ik_3z}, & z<0\ ,\end{cases} \tag{A6}$$

where

$$A_\sigma^{(1)} = \frac{1}{2}\left[1+\sigma\frac{k_0}{k_1}\right]\exp[i(k_0-\sigma k_1)(d+L)] \ , \tag{A7a}$$

$$B_\sigma^{(1)} = \frac{1}{2}e^{ik_0(L+d)}e^{-2\sigma k_2 d}\left[\left[1+\sigma\frac{k_0}{k_2}\right]\cos(k_1L) - i\left[\frac{k_0}{k_1}+\sigma\frac{k_1}{k_2}\right]\sin(k_1L)\right] \ , \tag{A7b}$$

$$\begin{aligned} T_\sigma^{(1)} = \frac{1}{2}e^{ik_0(L+d)}\Bigg[&\left[1+\sigma\frac{k_0}{k_3}\right]\cos(k_1L)\cos(k_2d) - i\left[\frac{k_0}{k_2}+\sigma\frac{k_2}{k_3}\right]\cos(k_1L)\sin(k_2d) \\ &- i\left[\frac{k_0}{k_1}+\sigma\frac{k_1}{k_3}\right]\sin(k_1L)\cos(k_2d) - \left[\frac{k_1}{k_2}+\sigma\frac{k_0k_2}{k_1k_3}\right]\sin(k_1L)\sin(k_2d)\Bigg] \ , \end{aligned} \tag{A7c}$$

$$E_y^<(Q_\parallel\omega|z) = \begin{cases} R_+^{(1)}e^{+ik_0z} + R_-^{(1)}e^{-ik_0z}, & z > d+L \ , \\ D_+^{(1)}e^{ik_1z} + D_-^{(1)}e^{-ik_1z}, & d < z < d+L \ , \\ C_+^{(1)}e^{ik_2z} + C_+^{(1)}e^{-ik_2z}, & 0 < z < d \ , \\ e^{+ik_3z}, & z < 0 \ , \end{cases} \tag{A8}$$

with

$$C_\sigma^{(1)} = \frac{1}{2}\left[1+\sigma\frac{k_3}{k_2}\right] \ , \tag{A9a}$$

$$D_\sigma^{(1)} = \frac{1}{2}e^{-i\sigma k_1 d}\left[\left[1+\sigma\frac{k_3}{k_1}\right]\cos(k_2d) + i\left[\frac{k_3}{k_2}+\sigma\frac{k_2}{k_1}\right]\sin(k_2d)\right] \ , \tag{A9b}$$

and

$$\begin{aligned} R_\sigma^{(1)} = \frac{1}{2}e^{-i\sigma k_0(L+d)}\Bigg[&\left[1+\sigma\frac{k_3}{k_0}\right]\cos(k_2d)\cos(k_1L) + i\cos(k_2d)\sin(k_1L)\left[\frac{k_3}{k_1}+\sigma\frac{k_1}{k_0}\right] \\ &+ i\sin(k_2d)\cos(k_1L)\left[\frac{k_3}{k_2}+\sigma\frac{k_2}{k_0}\right] - \left[\frac{k_2}{k_1}+\sigma\frac{k_1k_3}{k_0k_2}\right]\sin(k_2d)\sin(k_1L)\Bigg] \ . \end{aligned} \tag{A9c}$$

Finally, to construct $g_{yy}^{(0)}$ we require

$$\begin{aligned} W_\perp(Q_\parallel,\omega) = ik_0e^{+ik_0(L+d)}\Bigg[&\left[1-\frac{k_3}{k_0}\right]\cos(k_2d)\cos(k_1L) + i\cos(k_2d)\sin(k_1L)\left[\frac{k_3}{k_1}-\frac{k_1}{k_0}\right] \\ &+ i\sin(k_2d)\cos(k_1L)\left[\frac{k_3}{k_2}-\frac{k_2}{k_0}\right] - \left[\frac{k_2}{k_1}-\frac{k_1k_3}{k_0k_2}\right]\sin(k_2d)\sin(k_1L)\Bigg] \ . \end{aligned} \tag{A10}$$

---

*Permanent address: Instituto de Fisiĉa, Unicamp, 13100 Campinas, Brazil.

[1]John Lambe and S. L. McCarthy, Phys. Rev. Lett. 37, 923 (1976); S. L. McCarthy and J. L. Lambe, Appl. Phys. Lett. 30, 427 (1977); 33, 858 (1978); P. K. Hansma and H. P. Broida, Appl. Phys. Lett. 32, 545 (1978); and Arnold Adams, J. C. Wyss, and P. K. Hansma, Phys. Rev. Lett. 42, 912 (1979).

[2]We wish to thank Professor P. K. Hansma for providing us with a laboratory demonstration of this phenomenon.

[3]This saturation effect is discussed briefly by S. L. McCarthy and J. L. Lambe, Appl. Phys. Lett. 30, 427 (1977).

[4]The effect of surface roughness on surface polaritons has been discussed by D. L. Mills, Phys. Rev. B 12, 4036 (1975); A. A. Maradudin and W. Zierau, Phys. Rev. B 14, 484 (1976); and E. Kroger and E. Kretschmann, Phys. Status Solidi B 76, 515 (1976).

[5]A. A. Maradudin and D. L. Mills, Phys. Rev. B 11, 1392 (1975); D. L. Mills and A. A. Maradudin, Phys. Rev. B 12, 2943 (1975); G. S. Agarwal, Phys. Rev. B 14, 846 (1976).

[6]L. C. Davis, Phys. Rev. B 16, 2482 (1977).

[7]D. Hone, B. Mühlschlegel, and D. J. Scalapino, Appl. Phys. Lett. 33, 203 (1978); R. W. Rendell, D. J. Scalapino, and B. Mühlschlegel, Phys. Rev. Lett. 41, 1746 (1978).

[8]A. Dande, A. Savary, and S. Robin, J. Opt. Soc. Am. 62, 1 (1972).

[9]See, for example, the data on Au-Al_2O_3-Al junctions reported in Fig. 1 of J. Lambe and S. L. McCarthy, Phys. Rev. Lett. 37, 923 (1976).

[10]Our theory treats the roughness by perturbation theory, so the form for $l(\omega)$ that appears in the formulas is the mean free path on the smooth surface. This is finite because the dielectric constants of the substrate materials have nonvanishing imaginary parts.

[11]The discussion by Agarwal treats and cures a difficulty that appears in the paper by Maradudin and Mills cited in Ref. 5.

[12]D. J. Scalapino and R. W. Rendell (private communication).

[13]While a factor of the area of the junction appears explicitly in Eq. (2.42), it does not appear in Eq. (2.35) in an explicit fashion. However, upon tracing through the definition of $|\zeta(Q_{\parallel})|^2$, one sees that this quantity is proportional to the surface area. Thus, both Eq. (2.35) and Eq. (2.42) give total radiation intensities that scale directly with the surface area of the junction.

[14]The radiation which contributes to Eq. (2.42) is purely p polarized.

[15]See the paper by Maradudin and Zierau cited in Ref. 4.

[16]D. L. Mills and A. A. Maradudin, Phys. Rev. B 12, 2943 (1975).